UNIVERSITY OF MINES GHANA

PETROGRAPHY AND GEOCHEMISTRY OF IGNEOUS ROCKS IN AMOANDA DAMANG MINE AND IITS RELATIONSHIP WITH GOLD

By

GILBERT BIMPONG

(10361989)

THIS DESERTATION IS SUBMITTED TO THE DEPARTMENT OF EARTH SCIENCE OF THE UNIVERSITY OF GHANA LEGON IN PARTIAL FULFILLMENT FOR THE AWARD OF MSC MINERAL EXPLORATION.

MARCH , 2014

DECLARATION

This is to certify that this is the result of research carried out by Gilbert Bimpong towards the award of Master of Science in Mineral Exploration at the Earth Science Department, University of Ghana.

…….. Date……

Gilbert Bimpong

(Student)

…….... Date……..

PROF. P.M.NUDE

(Principal Supervisor)

…… Date…….

DR.C. ANANI

(Co-Supervisor)

ABSTRACT

Economic gold mineralization at Amoanda project area is hosted mainly in the footwall quartzite of the Banket series of the group. Igneous rocks generally are barren in both Amoanda project area and Greater Damang project area. However, core logs and sections from extensive deep drilling at Greater Damang has identified a deep-seated mineralized diorites body whereas igneous intrusive rocks in Amoanda which is suspected to be having similar characteristics show no gold mineralization so far. The question asked is whether the intrusives are the same for the two different project areas and if so why one is mineralized and the other not.

Two methods were employed, namely petrography and geochemistry

Petrographically, two uniquely weak foliated and fractured igneous rocks, the Meta Diorite and the Meta Dolerite. Major alteration minerals in the selected samples were the cubic pyrites whereas that of the mineralized was euhedral. Geochemically, the average abundance of trace elements such as As,Mn,Fe,Cu,Mg and Ag in selected igneous rocks which form pathfinders to gold mineralisationin in the Birimian were below the background values of average elemental abundance of As, Mn,Fe,Cu,Mg and Ag in normal igneous rocks. This suggests that the intrusives in the Amoanda project area is unmineralised according to Green (1959).

Structurally, deformation is weak in the unmineralised igneous rocks where deformations in the mineralized rocks are extensive. The extensive deformation of mineralized deep seated igneous rocks may be as a result of the presence of a structural regime that ruptured and provided enabling environments for the permeation, cooling and subsequent deposition of gold mineralization from the ore bearing hydrothermal fluids.

DEDICATION

Dedicated to my loving Parents, Mr. and Mrs.Bimpong, my siblings Theophilus, Nana Menu, Kwame Kusi,Isaac and Samuel for their unflinching support.

Lastly to Dr. Mike Affam for being a pillar in my career as a Geologist.

ACKNOWLEGEMENTS

"For All Things Work Together For Good To Those Who Love The Lord"

God's power, protection, sovereignty and mercies have seen me through this program successfully. And I am thankful to Him. To God be the glory, honour and adoration.

My profound gratitude goes to my academic supervisors, Prof. P.M. Nude and Dr. C.YAnani for their excellent guidance and for doubling as my parent throughout my academic work. I am so thankful for your support and encouragement. My heart-felt gratitude goes to my course coordinator, DrAsamoahSekyi, whose love and support has brought me this far.

I thank Daniel Kwayisi so much for his assistance during the data preparation and analysis. His immense support has brought me this far and I will forever be grateful Daniel Kwayisi.

To all my family members in and outside of Ghana, I acknowledge every bit of help you gave in my life. Special mention is made of Dr. Affam and Dr. Ewusi.

I would like to express my utmost and heartfelt gratitude to my wonderful parents and siblings for their spiritually and emotionally support throughout this programme. And to my wife to be Alberta Ekua Eshun, I say thanks for your understanding. God bless you!

TABLE OF CONTENTS

CHAPTER TWO

CHAPTER THREE

CHAPTER FOUR

LIST OF FIGURES

LIST OF TABLES

CHAPTER ONE

INTRODUCTION

1.1 BACKGROUND

The Ashanti belt of Ghana is a key district of gold mineralization in the Paleoproterozoic terrain of West Africa. The area considered in southwest Ghana is covered by lithologies of the volcanic-sedimentary Birimian Supergroup and the overlying clastic sedimentary Tarkwaian Group which were jointly folded and metamorphosed under Greenschist facies conditions during the Eburnean tectonothermal event at about 2.1 Ga. Regional foliation and sub-parallel shear zones hosting mesothermal gold mineralization developed during deformation coeval with metamorphism. Four major types of primary gold mineralization are present in the Ashanti belt: (1) mesothermal, generally steeply dipping quartz veins in shear zones mainly in Birimian sedimentary rocks, (2) sulfide ores with auriferous arsenopyrite and pyrite, spatially closely associated with the quartz veins, (3) sulfide disseminations and stockworks in granitoids, and (4) paleoplacers of the Tarkwaian Group.

The Damang Mining Lease covers 27,000 ha on the Ashanti belt which incorporates 4 key projects areas; Greater Damang, Greater Amoanda, Greater Rex and Bonsa. Drilling has for over 5 years not revealed any gold mineralization within the birimian rocks which happen to sit on the Ashanti belt of Ghana. A better understanding the factors can assist the company on the reason for the no gold mineralization on the Amoanda concession.

1.2 THE STUDY AREA SETTINGS

1.2.1 Location and Accessibility

The Damang Gold Mine is located in southwestern Ghana Tarkwa, near the southern end of what is commonly referred to as the Tarkwa Basin, 300 kilometers by road west of Accra, the capital of Ghana as shown in Figure 1.1). The area is served with good access roads and an established infrastructure. The Mine is further served by a main road connecting to the port of Takoradi, some 90 kilometres to the south-east. Damang Concession, which covers a total area of 27,174 ha, is located in the Western Region of Ghana , under a mining lease dated September 1996 for a term of 30 years commencing in 1996.

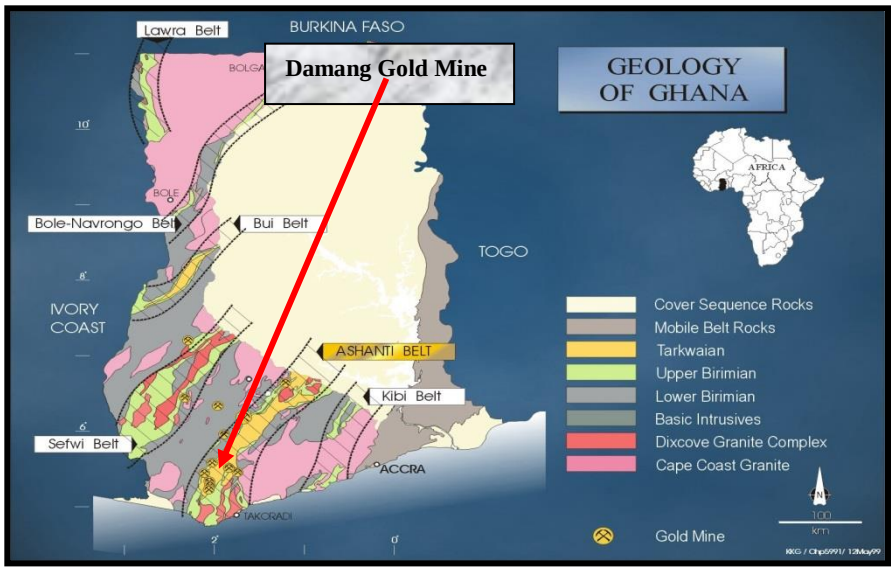

Figure 1.1: Geology of Ghana showing the location of Damang Gold Mine (anon., 2005)

1.2.2 Physiography

Damang Goldfields lies within the tropical region of Ghana with average monthly temperatures between 21°C and 32°C, is characterized by two distinct rainy seasons from March to July and September to November. Average annual rainfall near the site is 2,030 millimetres.

1.3 Problem Definition

Economic gold mineralization at Amoanda project area is hosted mainly in the footwall quartzite of the Banket series of the group. Igneous rocks generally are barren in both Amoanda and Greater Damang project area. However, core logs and sections from extensive deep drilling at Greater Damang has identified a deep-seated mineralized igneous intrusive body (assay results returned grades of 8g/t – 10g/t) as compared with 0.02-0.08g/t recovered from similar rock types at Amoanda. It is for this reason the current study is being undertaken to establish the factors responsible for gold mineralization in some areas and not in other areas o the same concession though the rock types are similar.

1.4 Justification of Study

Generally, igneous rocks encountered at the Damang project area are barren. Deep seated intrusive rocks at Greater Damang which are known to be the same rock as that outcropping in Amoanda is mineralized with Assay results of 8g/t-10g/t but that of igneous rocks in Amoanda is unmineralised. The reason for the no gold mineralization shown in Amoanda is yet to be investigated. The study, based on the findings will help the company to understand the factors contributing to the no gold mineralization in certain known intrusives which are mineralized elsewhere within its concession holdings.

1.5 Objectives

This research therefore seeks to answer the following questions:

(i). Are the intrusive petrologically the same?

(ii). If so, why is one mineralised with gold and the other barren?

(iii) If not, what are the differences between the intrusive types?

CHAPTER TWO

LITERATURE REVIEW

2.1 REGIONAL GEOLOGY

2.1.2 The West African Craton

The West African craton (Figure 2.1) consists of two major basement domains of Archaean and Paleoproterozoic age, namely the Reguibat Rise in the north and the Leo Rise (Guinea) in the south. These domains are separated by the Proterozoic to Paleozoic sedimentary basin of Taoudéni and are entirely surrounded by Pan-African belts (Trans-SaharianMauritides and Rockellides). The Leo Rise may be divided into an Archaean portion in the west and a Birimian portion in the east. These domains are separated by the strike-slip Sassandra fault and shear zone and by an Achaean-Palaeoproterozoic transitional domain (Feybesse and Milési, 1994; Caby et al., 2000; Klein and Moura, 2008).

In the Reguibat rise, Archaean and Birimian systems are separated by the Zednes Fault in Mauritania. Similarly, in the Man rise, an important shear zone, the Sassandra Fault in Ivory Coast, separates the Archaean and Birimian formations (Boher et al., 1992). It has been suggested that only one shear zone extends under the Taoudéni Basin (Caen-Vachette, 1988). However, no Archaean formations outcrop in the Precambrian inliers of Kedougou-Kenieba and Kayes (Bassot, 1963; Bassot and Caen-Vachette, 1984) which could attest to the continuity between the Man shield and the Amsaga domain. Generally, the WAC has been characterized by a complex polycyclic structural history, as indicated by numerous folds and faults. Figure 2.1 shows geological setting of West Africa (adopted from Feybesse et al., 2006).

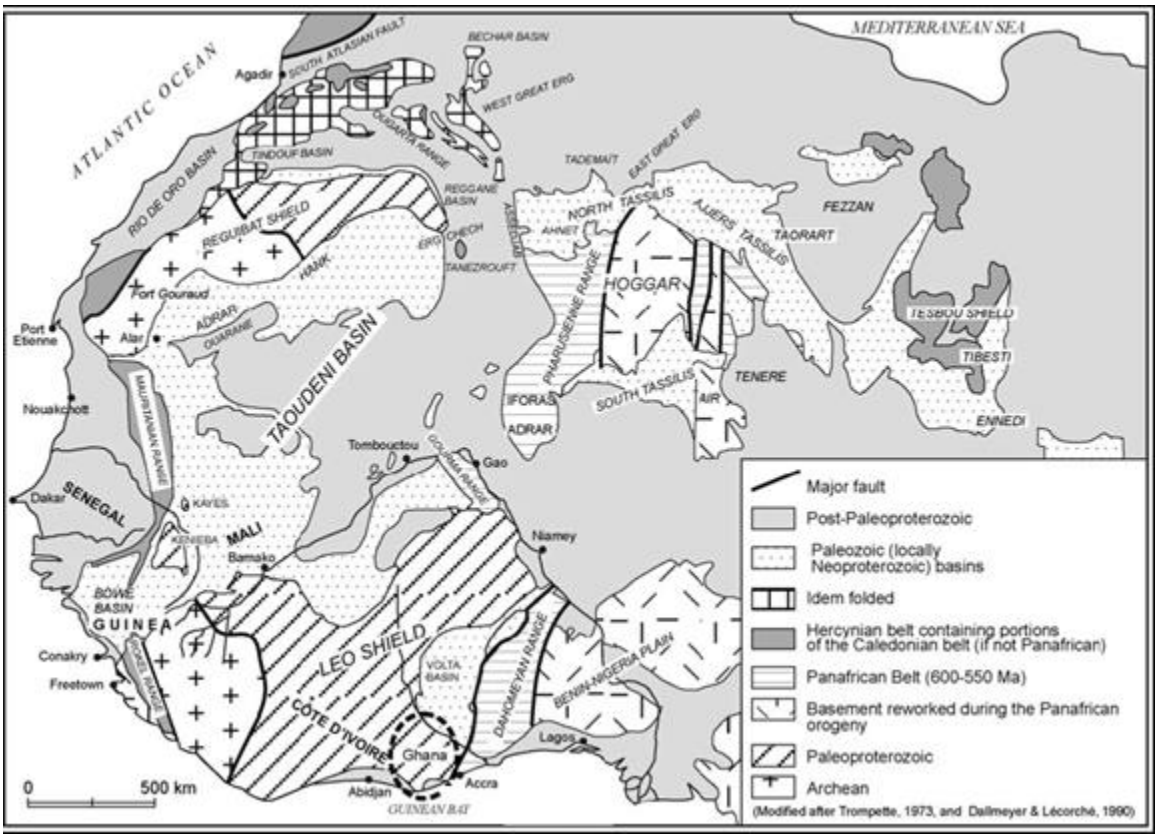

Figure 2.1 shows geological setting of West Africa (adopted from Feybesse et al., 2006).

2.1.2.1 Archaean domain

The Archaean formations are located in the western part of the WAC, where they form the Tiris-Amsaga nucleus (in Mauritania) and the Man nucleus (in Cote d'Ivoire, Liberia, Sierra Leone and Guinea). The formations are made up of extensive granite-gneiss complexes and greenstone belts enclosing basic and ultrabasic rocks and iron-bearing formations. The gneissic complexes predominantly consist of granulitic and magmatitic rocks, which are sometimes foliated. Amphibolites and metasedimentary rocks are locally associated with the gneisses (Junner et al., 1940).

The Archaean greenstone belts are made up of an assemblage of tholeiitic volcanic-plutonic rocks, and volcanic and sedimentary rocks. Ultramafic lavas, tholeiitic basalts, gabbros, dunite and chromite (which occur in layers) are present in the greenstone-granite terranes. The metavolcanic formation may be characterized by amphibolites with subordinate serpentinite, quartzites and banded iron formation (BIF) horizons. The BIF

horizons, however, predominantly occur in the metasedimentary units. Iron oxides comprise the iron formations, and usually occur as banded quartzite, meta greywacke and schist (Hirdes et al., 2004).

2.1.2.2 The Paleoproterozoic 'Birimian' terrane

Paleoproterozoic rocks, which comprise the bulk of the Birimianterrane of the Leo-Man shield (Fig. 2-2), form a significant portion of the West African Craton (Bessoles, 1977) to the east and north of the Archaean Liberian cratonic nucleus (Camil, 1984). The Birimianterrane or Eburnean province (also referred to as Baoulé–Mossiterrane by some geologists) underlies parts of Ivory Coast, Burkina Faso, Mali, Niger, Guinea, Liberia and Ghana. The Paleoproterozoicterrane is characterized by narrow sedimentary basins and linear and accurate volcanic belts intruded by several generations of granitoids (Leube et al., 1990; Pons et al., 1995; Hirdes et al., 1996; Doumbia et al., 1998), and corresponds to a period of accretion during the 2.1–2.0 Ga Eburnean orogeny (Bonhomme, 1962; Abouchami et al., 1990; Liégeois et al., 1991; Boher et al., 1992;Taylor et al., 1992).Figure 2.2 shows a geologic sketch of the Leo-Man shield of the West Africa craton (WAC; inset) showing the Paleoproterozoic (Birimian) greenstone belts (adopted after Attoh et al., 2006).

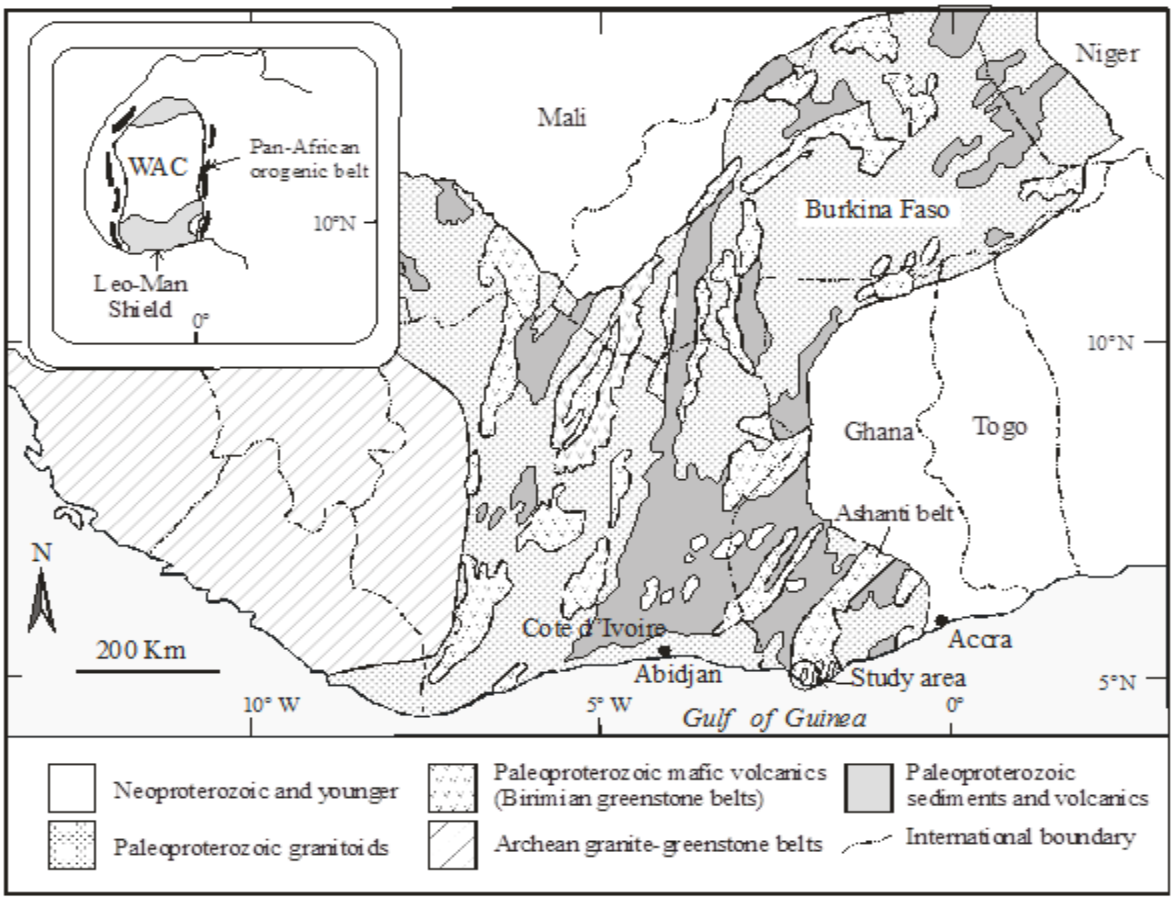

Figure 2.2 shows a geologic sketch of the Leo-Man shield of the West Africa craton (WAC; inset) showing the Paleoproterozoic (Birimian) greenstone belts (adopted after Attoh et al., 2006).

The accretion wasaccompanied by the deformation and the emplacement of syn- to

Post-orogenicgranodiorite–tonalite–trondhjemite (TTG) and granite plutons along fractures and by diapiric ascent (e.g., Leubeet al., 1990; Vidal and Alric, 1994; Feybesse et al., 2006). 207Pb/206Pb and U–Pb zircon geochronological data concerning the granitoid emplacement broadly cluster into two age groups (Hirdes et al., 1996; Doumbia et al. 1998; Hirdes and Davis 2002). The first group (2190–2108 Ma) occurs at the eastern subprovince of the Birimianterrane which includes Ghana, eastern Cote d'Ivoire and eastern part of Burkina Faso, whereas the second group (2110–2080 Ma) occurs at the west of the domain (which covers central and western Cote d'Ivoire, western Burkina Faso, Guinea and Mali). These coeval plutonism and volcanism are considered to mark two successive major episodes of Paleoproterozoic crust formation in the West African

craton. However, the occurrence of some pre-Birimian ages in detrital zircons (2245–2266 Ma) from the Tarkwaian sediments (Davis et al., 1994; Loh and Hirdes, 1999), in two zircon grains (2208 and 2220 Ma) from the Tafolo tonalite (Doumbia et al., 1998), in zircon cores from the Issia granite (2212–2305 Ma) in southwestern Cote d'Ivoire (Kouamelan, 1996; Kouamelan et al., 1997a), and in zircon cores from the Dabakala tonalite (2312±17 Ma; Gasquet et al., 2003) could probably suggest a pre-Birimian crustal growth episode. The Eburnean tectono-thermal event also resulted in widespread metamorphism mostly under the greenschist-facies conditions.

2.1.2.3 Geology and lithostratigrahic successions

The Birimian rocks were first termed "Birim Series" by Kitson (1918) to define a series of auriferous sediments from a type locality in Eastern Region of Ghana, the Birim River Valley. It was later changed to Birimian System to conform to the observations made in the field (Kitson, 1928; Junner, 1940; Asihene and Barning, 1975; Kesse, 1985). According to the definition of Cahen et al. (1984), the so-called Tarkwaian Group can be considered as part of the so-called BirimianSupergroup. The Birimian is believed to have accumulated in basins that developed on the Archaean crust. Thus, the Birimian was probably continuous with the Liberian basement exposed in the Archaeancratonic nuclei to the west (Petters, 1991). However, no evidence of direct contact exists between the Birimian and its presumed Archaean crystalline basement. Nevertheless, certain features of the Birimian may be used as indirect evidence for the presence of Archaean basement beneath the Birimianterrane. These include (i) the contrasting deformation and metamorphic styles between the Birimian supracrustal rocks and the surrounding crystalline rocks, and (ii) the nature of the clasts within Birimian basal conglomerates in parts of Ivory Coast and Burkina Faso, which might indicate that the Birimian was partially derived from and deposited on Liberian-age basement gneisses and migmatites (Petters, 1991).

The lithostratigraphic succession of these Paleoproterozoic rocks has over the years witnessed opposing views. According to some workers (e.g., Junner, 1940; Milési et al., 1992; Feybesse and Milési, 1994), the sedimentary unit is older than the volcanic unit, whereas other workers (e.g., Tagini, 1971; Hottin and Quedraogo, 1975;

Hirdes et al., 1996; Pouclet et al., 1996; Asiedu et al., 2004) believe that the volcanic unit is rather older. Lack of diagnostic field relationships between Birimian volcanic rocks and sediments is partly responsible for the controversy. Leube et al. (1990) have proposed a new version of the Birimian stratigraphy to partly harmonize the opposing views, where the two units formed quasi-contemporaneously as lateral facies equivalent.

2.1.2.4 Metamorphism

The Eburnean tectono-thermal event led to widespread deformation and metamorphism, resulting in a complex of northerly-trending shear zones in western Burkina Faso and Ivory Coast, and NE–trending shear zones in Ghana and eastern Burkina Faso. Metamorphism is mostly under the greenschist-facies conditions (Bessoles, 1977; Liégeois et al., 1991; Taylor et al., 1992; Bossière et al., 1996;Hirdes et al., 1996; Vidal et al., 1996; Doumbia et al., 1998; Oberthür et al., 1998; Béziat et al., 2000). However, evidence of medium amphibolite–facies metamorphism may be observed in the vicinity of granitoid plutons (e.g., Junner, 1935, 1940; Woodfield, 1966; Moon and Mason, 1967; Eisenlohr and Hirdes, 1992). Recently, John et al. (1999), on the basis of mineral chemistry, have suggested that the entire Ashanti belt of southeastern Ghana underwent epidote–amphibolite–facies metamorphism (T = 500–650 °C and P = 5–6 kbar) before experiencing retrograde metamorphism under the greenschist-facies conditions. Debat et al. (2003) have described the occurrence of amphibolite–facies assemblages, especially the kyanite–staurolite (Ky-St) pair, in Paleoproterozoic rocks in the Arbinda area of Burkina Faso. According to the authors, it is rare to find a Ky–bearing assemblage unambiguously associated with contact metamorphism; the Arbinda situation/aureole is probably the third world occurrence (after the Kwoiek aureole in British Columbia and of the Caplongue aureole in the French Massif Central) of a metamorphic–assemblage sequence where kyanite occurs above the staurolite isograd in the granitic aureole, according to the definition of Pattison and Tracy (1991). Debat et al. (2003) have also suggested that the Birimian crust in the north and central Burkina Faso and Niger shares similar characteristics with the Archaean in geodynamic context, where there is a common occurrence of staurolite and kyanite-bearing assemblages around granite batholiths.

2.1.2.5 Tectonic setting

Tectonic evolution models erected for the Paleoproterozoic rocks of Ghana have commonly invoked two deformation events. In the first event, the Birimian rocks were deformed and intruded by granitoid, and was later uplifted and eroded. The erosional products deposited in a series of grabens located within the volcanic belts to form the Tarkwaian. During the second event, which involved renewed folding (cf. Moon and Mason, 1967; Ledru et al., 1988) or gravity tectonic processes (Leube et al., 1990), both the Birimian and Tarkwaian were deformed. Recent structural data, however, suggest that both Birimian and Tarkwaian were subjected to a single, progressive deformation event, which involved compression along a southeast-northwest trending axis, resulting in folding and thrusting with subsequent flattening and localized oblique-slip shearing (e.g., Eisenlohr and Hirdes 1992; Blenkinsop et al., 1994).

Like other Paleoproterozoic terranes in West Africa, the tectonic setting of the Paleoproterozoic rocks of Ghana is contentious. One of the popular views is the tectonic model proposed by Leube et al. (1990). According to the authors, the tectonic evolution of the Birimian involved small-scale, equidimentional, parallel and contemporaneously operating convection cells in the upper mantle which caused a pronounced attenuation of an Archaean sialicprotocrust, followed by the rifting of a highly thinned protocrust as well as linear eruptions of N-MORB tholeiitic magma. With the growth of the volcanoes above sea level, volcanogenic sediments accumulated in the slowly subsiding parallel basins. After cessation of the volcanic activity and lateral compression generated by two adjacent contracting sialic blocks, crustal shortening and folding resulted, leading to the emplacement of the Baoulé type granitoids. The final stage in the evolution of the Birimian belt was caused by the reactivation of rifts and the formation of intra montane basins in the volcanic belts. The Tarkwaian molasse represents the infilling of these later basins with clastic sediments that were derived from Birimian rocks eroded nearby. This was followed by gravity deformation of Tarkwaian sediments, and by the intrusion of mafic sills and post-Eburnean Bondoukou or Dixcove type K-rich granitoids. Thus, the authors suggested an evolution of the tectonic setting of the Birimian/Eburnean in Ghana from an intracratonic-rift to

oceanic-spreading and finally to an accretion-collision-related setting. Alric (1990) has also proposed that the Birimian greenstone belts formed in intracontinental rifts.

On the basis of isotopic data and occasional presence of calc-alkaline andesite-dacite-rhyolite sequences, Pohl and Carlson (1993) have suggested that the Birimian volcanic belts mostly represent island arc complexes and some are external back-arc basins. The authors have indicated that the crustal shortening period of the Birimian involved a closure of an oceanic basin (located between the Man shield and the Nigeria craton) where multiple arc-arc collisions or, in the west, arc-continental platform collisions took place. Pohl and Carlson (1993) have also compared the Birimian situation to the compression of the Indonesian-Melanesian Archipelago and the intervening basins by the northward migration of the Australian plate towards the Asian continent.

Sylvester and Attoh (1992), drawing largely from the trace element geochemistry of the Birimian volcanic rocks in Ghana, coupled with (i) basaltic–andesitic–dacitic pyroclastic rock association in the greenstone belts, (ii) occurrence of andesitic and dacitic pyroclastic rocks together with volcanogenic sediments including fine-grained, fragmental volcanic rocks in the sedimentary basins, and (iii) the association of chemical sediments (i.e., manganese stones and chert) with the volcanic rocks, have indicated that the Birimian greenstone belts formed in oceanic island arc environments similar to those inferred for the Late Archaean Superior craton.

Davis et al. (1994) have also indicated the similarities in regional geological patterns and relative internal age relationships between the Paleoproterozoic Eburnean orogen of Ghana and the late Archaean Kenoranorogen of the southern Superior Province in Canada. In the southern Superior Pronince of Canada, deposition of volcanogenic-turbiditic basin sediments is suggested to be synchronous with accretion of arcs and micro-continental fragments against a growing continental mass.

Loh and Hirdes (1999), largely based on field observation, low TiO2 contents as well as a calc-alkaline differentiation trend for basalts from the southern Ashanti belt, agree with Sylvester and Attoh (1992) that the Birimian rocks erupted in a primitive island-arc environment.

Asiedu et al. (2004) have indicated that metagreywackes and metapelites from the Birim diamondiferous field show geochemical signatures similar to their Archaean counterparts. According to the authors, the chemical data of the rocks suggest that the rocks were derived from the basaltic to dacitic volcanic rocks and grantoids within the Birimian greenstone belts, and were deposited in a tectonic setting comparable to modern island arcs.

Dampare et al. (2005) have indicated that the geochemical signatures of the I-type granitoids from the southern Ashanti belt are consistent with those of granitoids emplaced in volcanic-arc settings. Considering the fact that the belt granitoids and volcanic rocks of the Birimianterrane of Ghana are coeval (Hirdes et al., 1992; Davis et al., 1994), Dampare et al. (2005) prefer an island arc tectonic setting for the Birimian belts.

Feybesse et al. (2006), in their metallogenesis model for the occurrence of gold deposits in Ghana, have implied a combination of continental margin, juvenile magmatism and convergence and collision between an old continent and a juvenile crust for the tectonic environments in which the Birimian greenstone belts were generated.

The largest mafic–ultramafic complex in Ghana which crops out in the southern Ashanti belt (Loh and Hirdes, 1999) has recently been re-interpreted as a fragment of Paleoproterozoic ophiolitic complex emplaced in a supra-subduction zone (SSZ) tectonic setting (Attoh et al., 2006).

Also, Dampare et al. (in press) have, on the basis of geochemistry, inferred an intra-oceanic island arc–fore-arc–back-arc setting for the Paleoproterozoic metavolcanic rocks from the southern Ashanti volcanic belt.

Thus, interpretations of tectonic models for the Birimianterrane of Ghana basically vary between the intra-cratonic rift setting and island arc complexes. Sylveste r and Attoh (1992), however, disagree with the proponents of intra-cratonic rift setting (Leube et al., 1990) for the following three reasons: (i) there is no evidence for significant volumes of continental crust older than the greenstone belts in the Man-Leo shield (Taylor et al., 1988; Abouchami et al., 1990); (ii) mafic and felsic volcanic rocks are voluminous in many modern intracratonic rifts but have not been found among Birimian volcanic rocks; and (iii) modern rift-related

volcanic and sedimentary rocks have formed before and during external tectonism, whereas Birimian supracrustal sequences formed before and during compressional tectonism.

2.2. Economic geology

Paleoproterozoic rocks of Ghana are the main host of the country's major mineral deposits, which include gold, manganese, bauxite, diamond and iron. The majority of the gold deposits are located along the flanks of the Birimian volcanic belts; some also occur within the volcanic belts where they sometimes show a spatial association with the belt-type granitoids (i.e., Dixcove granite). Manganese is mostly located as the transitional zone between belt volcanics and basin sediments. Other chemical sediments, such as sulphides, cherts, Fe–Ca–Mg carbonates and rocks rich in carbon also occur at the transition zones along the flanks of the volcanic belts (Ntiamoah-Agyakwa, 1979). Diamonds have mostly been found from Birimian sediments as well as diamondiferous rocks.

2.3 GEOLOGY OF STUDY AREA

2.3.1 Local Geology

Damang is located on a regional anticline called the Damang anticline (Figure 2.4). The Tarkwaian stratigraphy is consistent along the east and west limbs of the Damang anticline. The Damang area is composed mainly of sedimentary rocks which have been intruded by igneous rocks and overlay a basal Birimianvolcanics and volcanoclastics rock package. Table 2.1 gives a detailed description of the major rock types (Sharp, 2005).

An angular unconformity at the base of the Tarkwaian separates it from the Birimian. The major difference between the east and west limbs of the Damang anticline as shown on Figure2.4 is the absence of the Kawere strata in the eastern limb (anon., 2005). The major lithologies in the Amoanda project area are the kawere which is found on the western side of the project area, the sandstone and the Birimian on the eastern side of the project area. Figure 2.3 shows photographs of Kawere and the footwall banket sandstone.

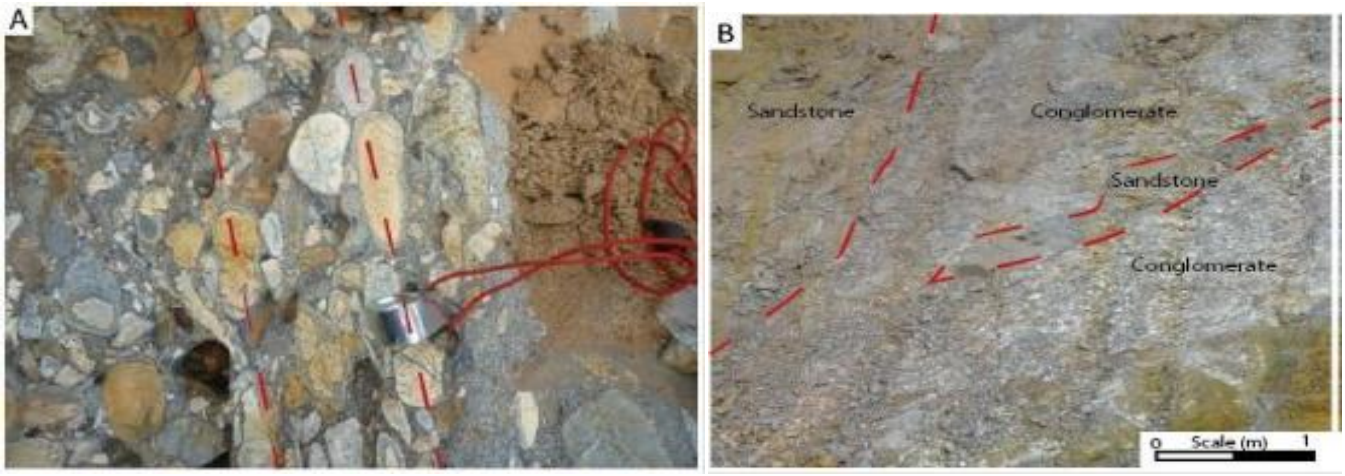

Figure 2.3: (A) An outcrop photograph of a Kawere conglomerate horizon showing NE-SWorientated elongation of the clasts lithic and quartz vein clasts. (B) An outcrop photograph showing sandstone on the project area.

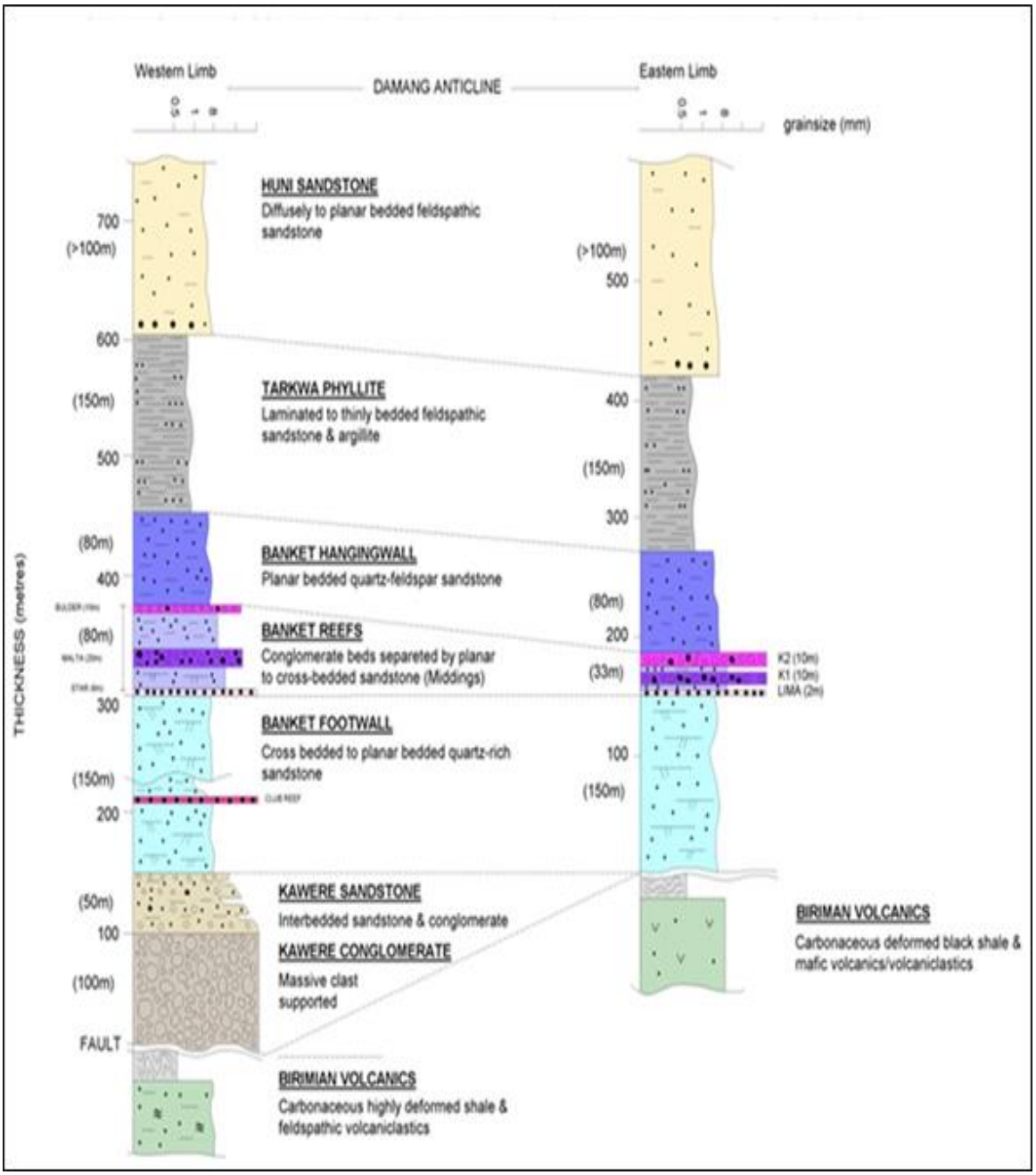

Figure 2.4 shows the geology of Damang along the limbs of the anticline (Sharpe, 2005).

Table 2.1: Description of the major rock types in Damang

Lithology		Description
Huni Sandstone		Diffuse to planar bedded feldspathic sandstone.
Tarkwa Phyllite		Very fine grained, metamorphosed mudstone to silty mudstone, which shows grading, lamination and soft sediment deformation and occasional graded beds up to 1m thick of fine to medium grained lithic arenites.
Banket Hangingwall quartzites		Comprises a fining upwards sequence of coarse to very coarse grained, sub-mature sandstone (lithic arenite) with thin, polymictic, medium to small pebble lags on scour surfaces towards the base. Both cross bedding and parallel stratification are present.
Banket reefs	**Gulder/K2 reef**	The reefs consist of very polymictic, poorly sorted, matrix supported very large pebble conglomerates showing mainly parallel stratification and sub-angular pebbles interbedded with parallel stratified and cross bedded very coarse grained sub-mature sandstones.
	Malta/K1 reef	Consists of a coarsening then fining upwards sequence of polymictic matrix supported, medium to large pebble and oligomictic, clast supported, small cobble conglomerates interbedded with cross bedded, coarse grained, mature sandstones.
	Star/Lima reef	A fining upward clast supported oligomictic quartz pebble rich unit.
Banket Footwall quartzites		Comprises a monotonous succession of well sorted, medium to coarse grained, cross bedded sub-matured sandstones which show well marked concentrations of magnetite on their foresets.
Kawere	**Kawere sandstone**	Interbedded sandstones.
	Kawere conglomerate	Massive, clast supported conglomerate.
Birimian		Consists of carbonaceous, highly deformed shale (volcanics) and feldspathic volcaniclastics.

2.4 MINERALISATION

2.4.1 Palaeoplacer Mineralisation

There are three gold-bearing conglomerate horizons recognized on the western limb of the Damang anticline. From footwall to hanging wall, these are known as the Star/ Composite, Malta/Breccia and Gulder Reefs. There are also three gold-bearing conglomerate horizons recognised on the eastern limb, namely the Lima, Kwesie-K1 and Kwesie-K2 Reefs. These conglomerate horizons are separated by poorly-mineralised sandstone units.The

reefs are usually characterised by a fining upwards sequence of poorly to moderately sorted, clast-supported polymictic conglomerates (competent person's report). However, local variations are observed where the conglomerate domain is interbedded with fine to coarse grained, poorly sorted sandstones. The Star/Composite, Malta/Breccia and Gulder Reefs on the west limb and the Lima, Kwesie-K1 and Kwesie-K2 Reefs on the east limb of the Damang anticline contain higher gold grades than the poorly mineralised sandstone units, which separate the reefs. The conglomerate reefs may contain between 1.3 and 1.5 g/t gold, and the poorly mineralised sandstone units usually contain between 0.1 and 0.2 g/t gold (sharp, 2005).

2.4.2. Hydrothermal Mineralisation

Hydrothermal gold mineralisation at Damang occurs in pyrite and pyrrhotite alteration selvages, which are usually less than one metre wide and located immediately adjacent to en-echelon quartz veins. Gold is also associated with accessory vein minerals such as carbonate, muscovite, tourmaline, ilmenite and apatite. These alteration zones are often linked and may result in significant volumes, characterised by intense veining and gold mineralization (anon., 2005).

2.4.3 Geochemistry

Host rocks at Damang exhibits a number of types of alteration. A pervasive pink alteration is widespread in the Huni-sandstone has also been occasionally observed in the banket sandstone and meta-dolerite. Pink colouration is caused by a matrix of hematite-stained albite, oxidizing fluids. Similar alterations of sandstones is observed much farther south at Tarkwa, where no hydrothermal gold mineralisation is apparent, indicating that this alteration is a regionally extensive phenomenon unrelated to gold mineralization (anon.,2005).Meta-dolerites also show as much more localized bleaching caused by development of dominant carbonate and lesser sericite and chlorite and accessory leucoxene. Such bleached zones are commonly mineralized, though the dominant sulphide is usually pyrite rather than pyrrhoitite. The style of alteration is similar to that accompanying many Achaean basaltic-hosted gold deposits in greenschist facies terrains and is the result of reaction with strongly reducing fluids. Silicification and quartz veining are the most obvious widespread effects accompanying gold

mineralisation. Strong sericites alterations occur sporadically and appear most common in the highest grade intervals of sandstone and banket conglomerate. Mineralized dolerites, sandstones and meta-sediments also exhibit a range of alteration assemblages indicating reaction with moderately reducing fluids with varying sulphur fugacites. Intermediate alterations states retain pink albite and contain fresh magnetite in close proximity to domains of demonstrate overprinting of grey, mineralized vein selvages over the pre-existing oxidized assemblages. The majority of gold is intimately associated with pyrite-pyrrhotite mineralization which occurs in selvages around quartz veins. The veins themselves rarely contain sulphides, showing only trace amounts of carbonates, muscovites, tourmaline and illeminite (Anon., 2005).

CHAPTER THREE

METHODOLOGY

4.1 PETROGRAPHY

Two methods were used namely, Field method and Laboratory method.

4.1.1 Field Methods

4.1.1.1 Field mapping

4.1.1.2 Planning

Planning was done to deduce;

- Number of samples to collect
- Estimated duration of project
- Estimated cost of labour and equipment.

At the office, the known Universal Transverse Mercator (UTM) values were loaded onto the GPS (Geographical Positioning System) and whiles on the field, these point served as a bench mark from which the bearing of the rock types were taken.

Prior to the knowledge on the general trend of the anomaly established from the stream sediment sampling, surveyors establish the NE-SW direction using the theodolite.

4.1.1.3 Pit Mapping and Outcrop mapping

Pit mapping was also conducted in the Amoanda pit. Steeply (vertical in some instances) dipping dykes of pale to dark grey igneous intrusive rock units were identified.

4.2 Data collection

Generally there is a scarcity of outcrops on the Amoanda property which is largely due to the intense weathering and thick vegetation coverage. Where an outcrop is present it is characterised by a thick oxide and overburden horizons of some 20m-35m. To overcome this challenge mapping was conducted along recently constructed roads, in ponds, on erosional surfaces and on farms. Most of the exposures had somewhat been weathered due to the long exposure periods. This made it difficult to get attitude measurements and select relatively unaltered and fresh samples for thin section analysis. This challenge was overcome by selecting samples from drill holes that was deemed representative on the eastern side of the project area.

4.2.1 Core Sampling and Preparation

4.2.1.1 Core Sampling

In order that representative samples were obtained for further study and analysis, drill cores were carefully selected.

4.2.1.2 Core logging

Geology, structures, weathering and alterations were logged from the study of these drill cores. This was done in order that the properties of drill core could be determined through hand specimen observation.

In all, Twenty five (25) diamond drill core were logged and only six drill holes returned representative intersections of igneous rocks. Below shows information on locations of drill holes sample in table 3.1 and a map showing the location of Amoanda project area.

Table 3.1 Location of sample drill holes.

PROSPECT	HOLEID	DEPTH_M	DRILL_TYPE	EAST	NORTH	RL
Amoanda	ANDD036	322.9	Diamond Drill	8622	19110.5	979.36
Amoanda	ANRC227D	216	Diamond Drill	8480	18864.3	992.77
Amoanda	ANRC228D	209	Diamond Drill	8452	18866.2	991.59
Amoanda	ANRC230D	235.1	Diamond Drill	8504	18943.1	990.73
Amoanda	ANRC231D	230	Diamond Drill	8480	18943.7	990.441
Amoanda	ANRC232D	270	Diamond Drill	8533	19030.1	1000.51

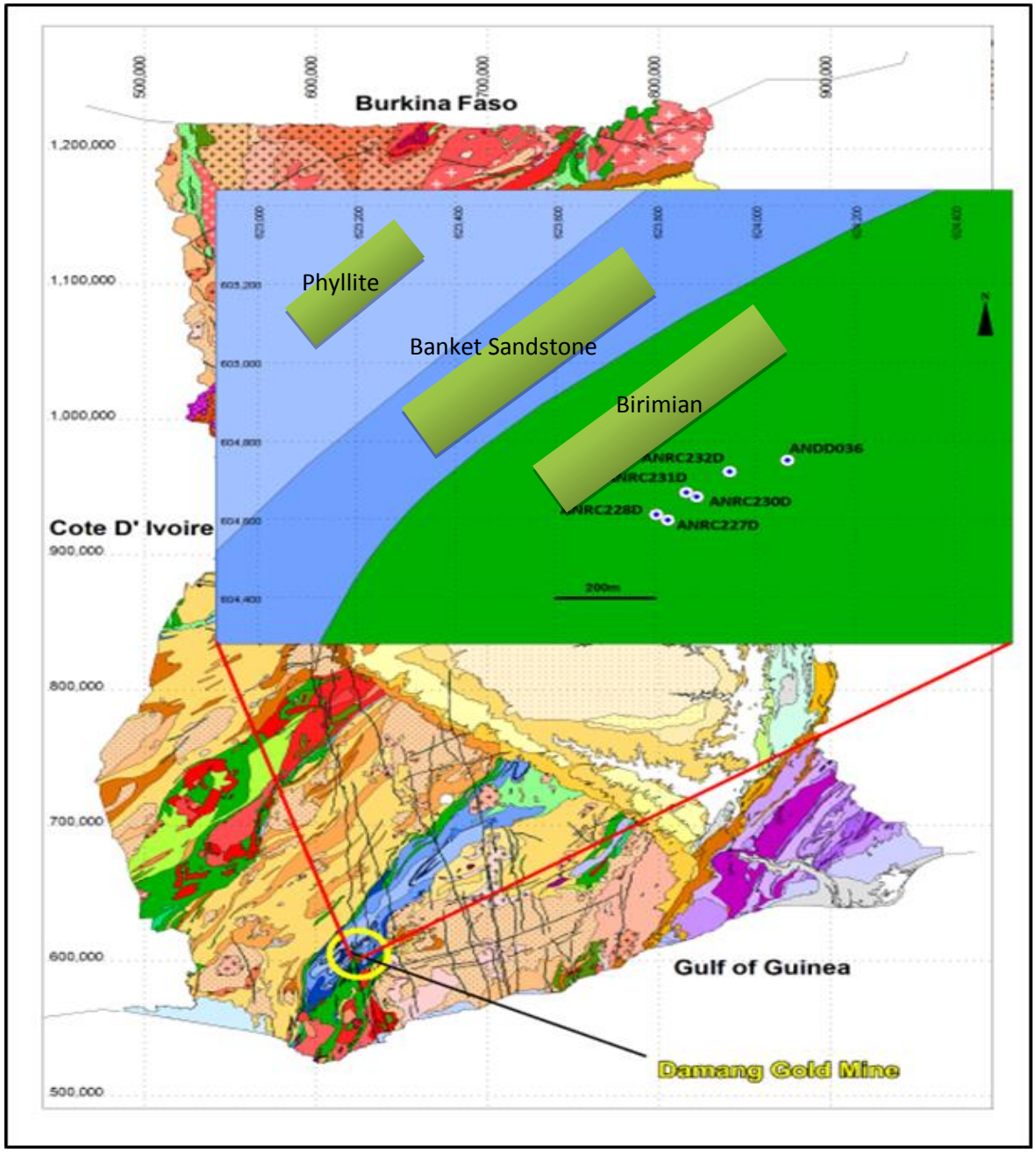

Figure 3.1: A map showing study area (sharp, 2005)

3.2 LABORATORY WORKS

3.2.1 Petrography

Six (6) half core samples were selected for the petrographic analysis to determine their mineralogical composition at the Geology laboratory of the University of Ghana, Legon, Accra.

3.2.1.1 Preparation of thin sections

Thin sections were prepared from the selected rock samples by first cutting and trimming the samples into slabs suitable for mounting. In order to achieve a flat reference surface, the slabs were manually lapped and grinded progressively (using 180, 240, 400, 800 and 1,200 mesh sizes). This was done in increasing order of grit size.

One of the faces of the specimen slab was then manually lapped flat and parallel on a glass plate using silicon carbide abrasive powder after the other face was labeled with an appropriate number. Small fragments of the rock samples were cut using a diamond saw. The fragments were ground flat and smoothed on one surface using silicon -carbide powder, starting with 80 grades and finishing with 600 grades. The smoothed surfaces were mounted on glass slides (usually 3" x l using Canada balsam. The other surfaces were then ground down until the rock section was 0.03 mm thick. Progressively finer abrasives were used as the section became thinner, and finishing was done with 600-grade carborundum powder. The thickness was gauged by observing the interference colors of common minerals such as quartz or feldspar.

After cleaning excess cement from the sections, they were covered with a glass cover-slip cemented with Canada balsam.

3.2.1.2 Thin Section Examination

Examination of thin sections under the microscope was performed to aid in the identification of minerals and micro-structures which were not identified with the naked eyes.

Plagioclase had low relief, lack of colour, biaxial character and polysynthetic (repeated twinning), with maximum interference colours in thin sections being first order gray or white. Muscovite was clear under PPL but with perfect cleavage and bright interference colours. It was distinguished from biotite by its lack of colour. A distinctive character is its pebbly surface. Cleavage is roughly parallel to thin section. Biotite was pleochroic with one perfect cleavage, strong natural colour masking polarisation colours to make it look greeneish under XPL. Amphibole was pleochroic with 2 cleavages at 60^{o} or 120^{o} distinguishing it from biotite or pyroxene. The distinguishing features of pyroxenes were its well formed crystal seen with 2 cleavages at 90^{o}. Calcite showed both high and low relief. Under XPL, calcite showed cleavages at 120^{0}. The common minerals observed in the mafic igneous rocks were mainly quartz, plagioclase, pyroxene and epidotes. Modal percentages of the minerals under thin section were estimated by the use of the visual estimation charts. Photomicrographs were then taken of each thin section examined. From the hand specimen and modal analyses, correct rock names were assigned to the various lithologies encountered in the field.

3.2 Geochemical Analysis

3.2.2 Chemical analysis

Half core elements analysis of 6 samples were performed at the ALS laboratory in Vancouver, Canada through ALS laboratory at New Brofuyedur, Kumasi in Ashanti region carried out by multi elements fusion inductively couple plasma mass spectrometry(ICP-MS).

3.2.2.1 Sample preparations

After the field work and petrographic studies, 6 representative samples were taken for geochemical analysis to determine their chemical compositions. These samples were crushed with harmer and further with an electronic crusher, pulverized and then sieved using 500µm mesh to obtain powdered samples for the chemical analysis. Before preparation, samples were washed in distilled water followed by ethanol and dried in sun for four days to remove any stains. The dried samples were wrapped in plastic zip lock bags with the sample IDs written

boldly on them. The samples were then crushed into smaller fractions of about 30 mm in diameter and further into sizes of about 5 mm in diameter. These small splintered rock-chips were finally taken and pulverized into smaller sizes using an agate mortar. The samples were finally sieved to obtain the powder.

To avoid cross contamination of samples, the pestle and the mortar used were cleaned between samples using acetone. An acetone-cleaned plastic spatula was used for transfer of pulverized samples from the mortar to sample containers between samples. Whole rock elements analyses of 6 selected samples were performed at the ALS laboratory in Vancouver, Canada, through ALS laboratory at New Brofoyedru, Kumasi in Ashanti region of Ghana. Major elements and trace elements analyses were carried out by multi elements fusion inductively coupled plasma mass spectrometry (ICP-MS). Loss on ignition was determined at 1000 °C. The detail analytical procedure is available at ALS laboratory.

3.2.2.2 Data Analyses.

Results from the field work and the laboratory work were presented in tables, compiled and plotted into graphs and maps using computer softwares such as Microsoft office suite, Mapinfo professional and SPSS.

CHAPTER FOUR

RESULTS AND DISCUSSIONS

4.1 Field Observations and Petrography

The six (6) samples were mafic composed mainly of plagioclase, pyroxene and quartz with sericites, cubic pyrites and muscovite as accessory minerals in general. Below shows various description of the rock types studied.

4.1.1 Rock Type Descriptions with Modal Composition

Sample ID	Mineral	Volume %	Rock
ANRC 238D	Chlorite	64	Meta Gabro
	Plagioclase	16	
	Pyroxene	10	
	Amphipbole	5	
	Sulfide mineral	3	
	Quartz	2	
ANRC 232D	Chlorite	45	Meta dolerite
	Epidote	40	
	Quartz	10	
	Plagioclase	3	
	Carbonate	1	
	Opaque	1	
DDD036	Quartz	35	Grano Diorite
	Muscovite	30	
	Sericite	25	
	Epidote	10	
	Opaque	<1	
	Carbonate	<1	
ANRC 227D	Plagioclase	45	Meta Diorite
	Altered amphibole	35	
	Quartz	25	
	Sulphide minerals	1	
	Epidote	5	
	Toumaline	<1	
ANRC 230D	Quartz	40	
	Epidote	35	
	Calcite	20	
	Sericite	4	
	Sulfide minerals	1	
	Toumaline	1	
ANRC 231D	Plagioclase	40	
	Pyronexe	35	
	Quartz	15	
	Opaque mineral	<1	
	Calcite	1	
	Tourmaline	1	

4.2 DESCRIPTIONS

The petrography studies identified four unique igneous rocks. Below is the detailed description of the rocks.

4.2.1 Meta Gabbro ANRC 238D

Sample ANRC238D in the area was generally dark green, coarse grained as shown in figure 4.1(A) and composed predominantly of chlorite and plagioclase with minor sulphides minerals, amphiboles and quartz which was recognized by its low relief, low birefringence and lack of cleavage in figure 4.1(B). Chlorite is somewhat fibrous and shredded with altered products of pyroxene and amphiboles. Chlorite is distinguished from other micas like muscovite and biotite by its color, pleochroism and weak birefringence. The groundmass of plagioclase is lath-like and significantly altered into sericite. Amphiboles are subhedral to anhedral. Sulphides minerals which are present as a result of metamorphism are cubic and looked deformed. This rock is a mafic plutonic rock of gabbroic composition, now metamorphosed to green schist facies. The rock may be Meta gabbro. Figure 4.1 (A) and (B) shows a core sample photograph and photomicrograph of sample ANRC 238D.

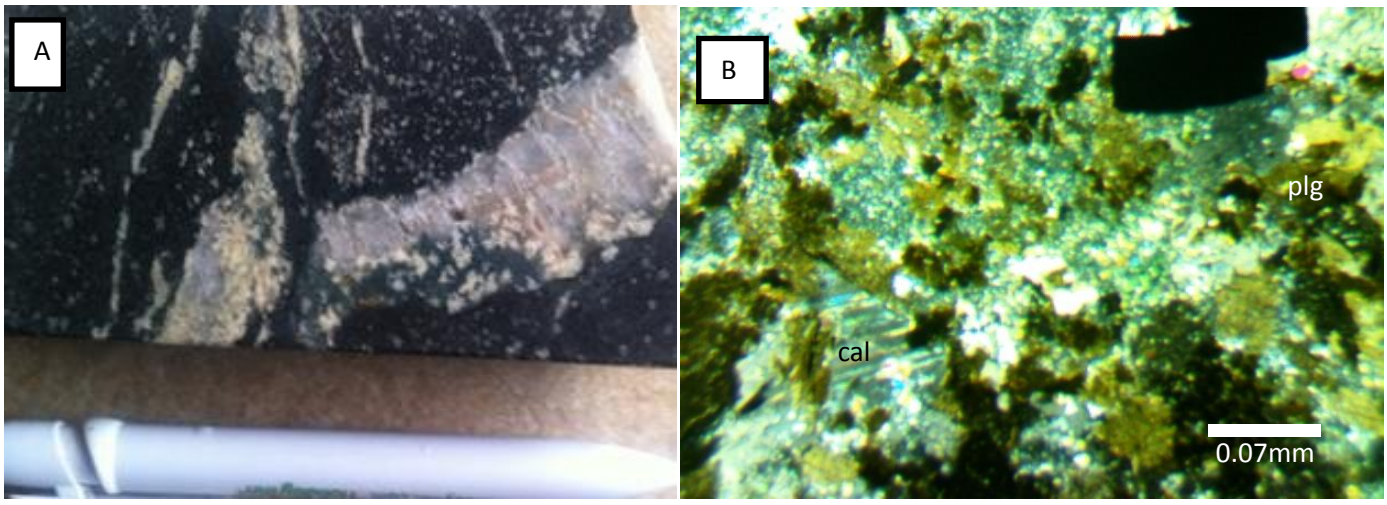

Figure 4.1 (A and B) shows photograph and photomicrograph of core sample ANRC 238D.

4.2.2 Meta Diorite

Samples ANRC 227D, ANRC 230D and ANRC 231D are considered to represent an intrusive mafic igneous rock which has been subjected to deformation and alteration. The original igneous rock was most likely to be a diorite although it could have originally been a gabbro. The alteration assemblage of these 3 samples consists of varying proportions of epidote, muscovite/sericite, toumaline and quartz. Although most of the quartz is thought to be an alteration product it is thought that some could represent remnant igneous quartz from a quartz diorite. Traces of tourmaline are also present in all 3 samples and are generally associated with the other alteration products. There are variations in the proportions of the alteration products in different samples with sample ANRC 227D having a high epidote content, sample ANRC 230D having a high sericite content and sample ANRC 231D having a higher quartz content. Rocks are medium to coarse grained and composed of plagioclase, amphiboles, quartz and epidotes with few occurrences sulphides and opaque minerals as accessory minerals. Plagioclase is colorless in thin section. Maximum interference colors in thin section are usually first-order gray or white. The low relief, lack of color, biaxial character, and polysynthetic twinning distinguish plagioclase from most other minerals. Untwined plagioclase greatly resembles quartz and may be easily overlooked. However, quartz is uniaxial and has no cleavage. Plagioclase is subhedral to euhedral porpheries and slightly altered to sericite in ANRC 230Dand ANRC231D. Plagioclase presents in ANRC 227D though partially sericitized have visible and good pseudomorphs. Quartz occurs as anhedral and crystalline, medium grained and exhibits undulose extinction. Sulphide minerals exhibits cubic to irregular shape that is deformed. Epidote appears shredded and probably an alteration product of the former ferromagnesian minerals. Calcite appears as isolated aggregates, might be probably secondary and interstitial in ANRC 230D &ANRC 231 but absent in ANRC 227D. These samples contain abundant intermediate minerals and may be an intermediate intrusive rock that is porphyritic. The pseudomorphs of these altered minerals are preserved in their alteration products. The rocks may collectively be named as diorite.

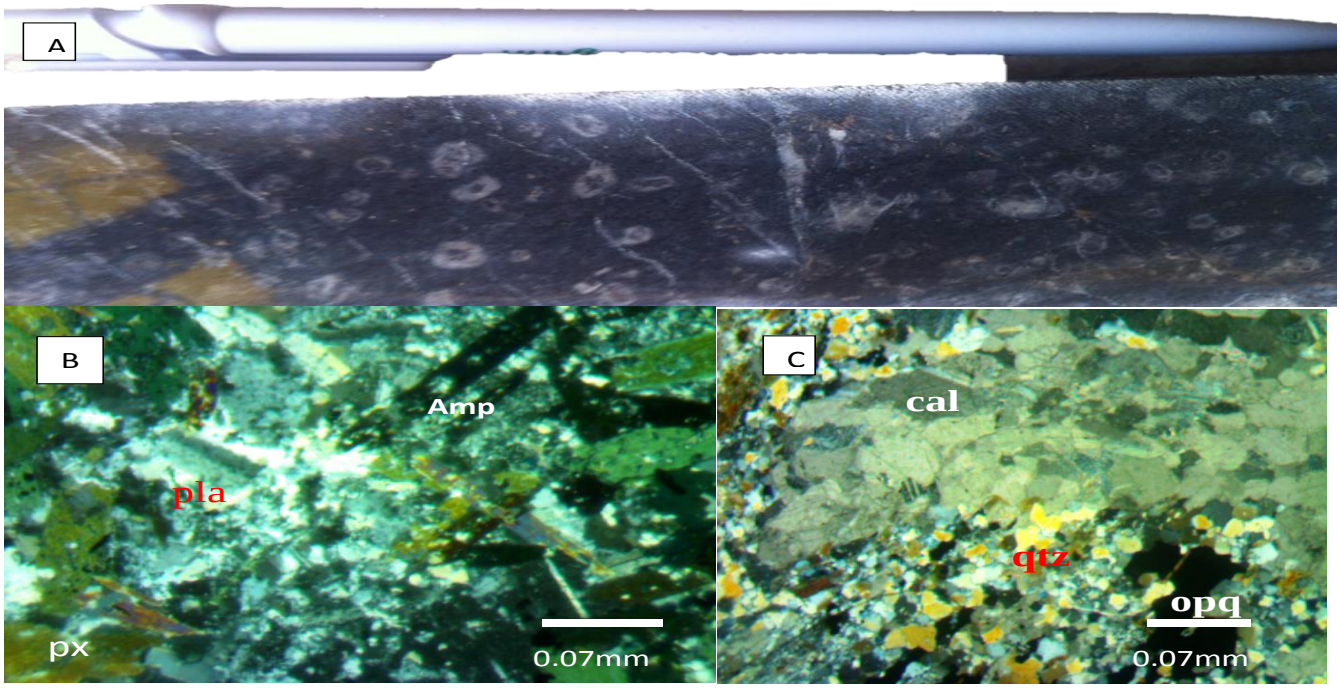

Figure 4.2: A photograph of core sample (A) and photomicrograph of sample ANRC230D &ANRC231D for specimen B and C respectively

4.2.3 Meta Dolerite-ANRC232.

The rock is fine to medium grained which are acicular, elongated and fibrous. Predominant minerals are chlorite and epidote with minor quartz, plagioclase, carbonates and opaque minerals. The opaque minerals are irregular, amorphous and therefore secondary and occur as smears on the chlorite. Chlorite appears fibrous and rims the quartz and plagioclase. Epidote appears elongated and acicular. These two minerals may have been altered from the primary ferromagnesian minerals such as pyroxene and amphiboles as pseudomorphs. The quartz displays undulatory extinction and some appear as turbid. Relative coarse plagioclase appears to be slightly altered to sericite.The rock may be sub volcanic of mafic composition preferably dolerite. Figure 4.3 (A) and (B) shows a core sample photograph and photomicrograph of sample ANRC 232D.

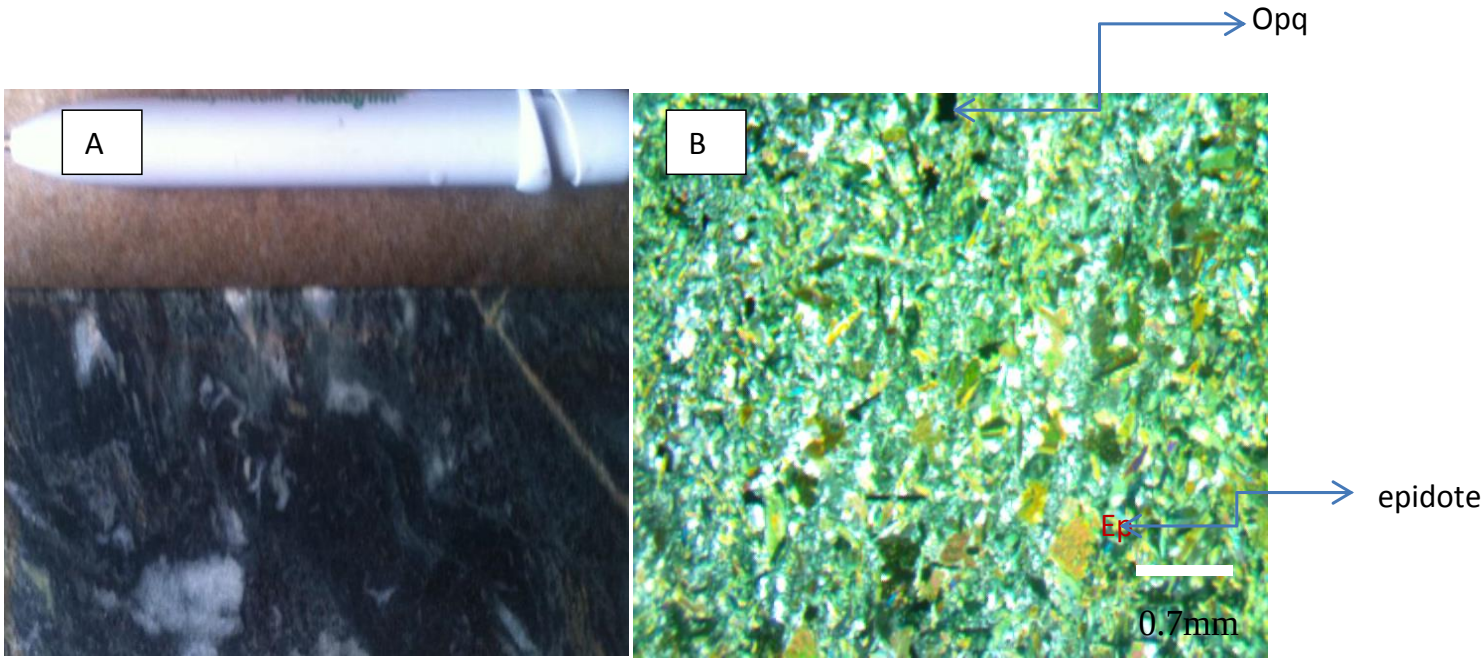

Figure 4.3 (A and B) shows photograph and photomicrograph of core sample ANRC 232D

4.2.4 Grano-Diorite-DDD036

The rock is medium grained, weakly foliated and composed of sericite, muscovite and epidote and quartz with few occurrences of carbonate and opaque minerals. The epidotes are shredded and appears altered from amphibole probably to hornblende. Quartz shows undulose extinction and occurs in the rock mass as its constituents minerals. Muscovite is thread like and rims the quartz. The sericite could be an altered product of plagioclase. Carbonate occurs only as veins and therefore could only be described as secondary. This rock is of a mafic precursor now metamorphosed. The rock may be epidote-sericite-muscovite schist. Figure 4.4 (A and B) shows photograph and photomicrograph of core sample ANDD036

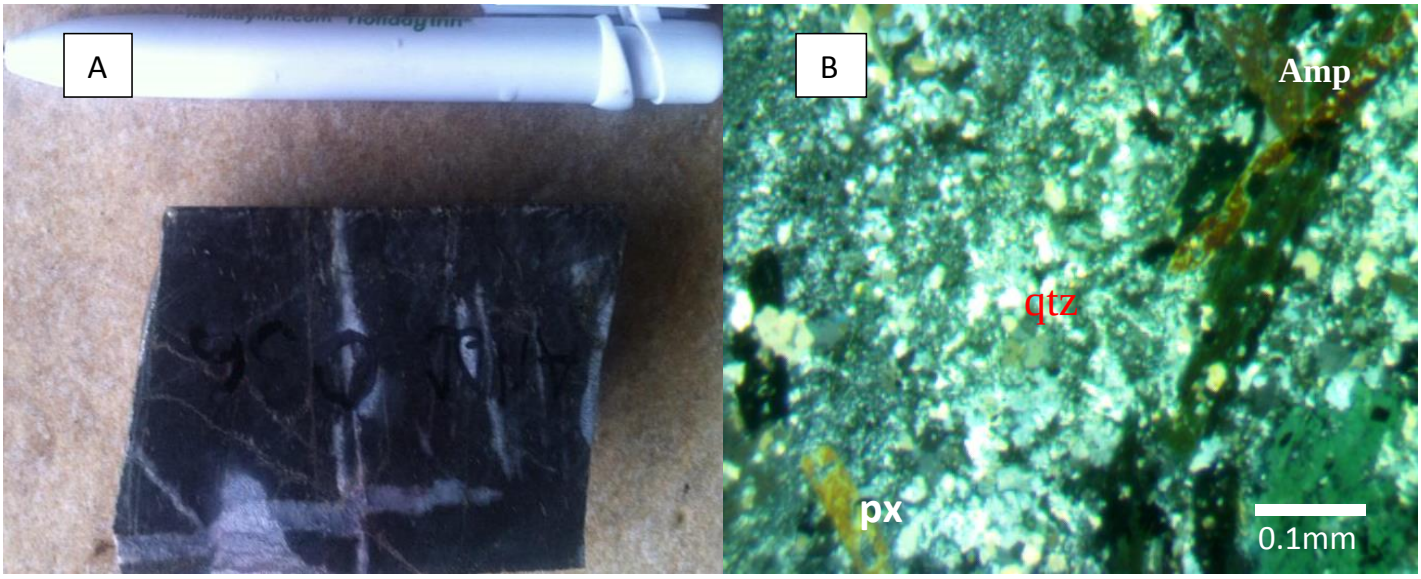

Figure 4.4 (A and B) shows photograph and photomicrograph of core sample ANDD036

4.3 Geochemistry

Mineralogical and geochemical studies conducted by Dzigbodi- Adjimah ,(1999) along the Birimian channel on the Ashanti belt shows that auriferous gold contains high trace element of Zn,Pb, Cu,Fe,As, Sb,Mn and Cd. The result of this study is therefore to run a correlation graphical plot to determine how the major elements such as As, Ag, Mg, Mn, Cu and Fe are related to Au in the above samples. Below is a geochemical result from ALS, Vancouver and correlationplot in appendix 1 between the various pathfinders of gold and gold.

Table 4.5: Geochemical results of multi-element analyses from ALS, Vancouver, Canada.

	ANDD036	ANRC227D	ANRC232D	ANRC230D	ANRC228D	ANRC231D
Ag	0.13	0.2	0.06	0.06	0.14	0.06
Al	1.46	2.14	1.37	2.11	2.25	1.79
As	76.5	58.5	0.9	1.1	1.2	0.9
Au	<0.2	<0.2	<0.2	<0.2	<0.2	<0.2
B	<10	<10	<10	<10	<10	<10
Ba	130	190	50	410	140	<10
Be	0.13	0.14	<0.05	0.11	0.06	<0.05
Bi	0.36	0.43	0.12	0.1	0.12	0.05
Ca	3.47	5.08	4.56	1.96	3.81	4.4
Cd	0.07	0.1	0.03	0.03	0.07	0.03
Ce	25.2	4.46	2.18	40.5	3.41	4.22
Co	21.3	46.6	25.1	14.5	56.8	43
Cr	27	361	162	27	435	193
Cs	0.89	1.14	5.5	6.16	3.14	0.09
Cu	56.4	134.5	93.3	28.7	187	117.5
Fe	4.02	6.2	3.07	3.77	6.15	5.23
Ga	5.69	7	3.4	9.09	8.11	6.46
Ge	0.08	0.12	0.17	0.11	0.22	0.19
Hf	0.06	0.03	0.02	0.11	<0.02	<0.02
Hg	<0.01	<0.01	<0.01	<0.01	0.01	<0.01
In	0.027	0.035	0.015	0.029	0.055	0.017
K	0.39	0.5	0.57	1.57	1.29	0.01
La	12.8	2.2	0.8	19.4	1.2	1.6
Li	20.2	30.9	34.5	38.6	43.5	14.3
Mg	0.98	3.06	1.84	1.44	3.39	2.49
Mn	1140	1080	755	853	802	828
Mo	1.21	4.44	8.58	0.69	9.71	0.13
Na	0.04	0.03	0.07	0.05	0.04	0.04
Nb	0.12	<0.05	<0.05	0.16	<0.05	<0.05
Ni	22.7	147	70.7	13.9	185	127
P	420	200	240	830	240	230
Pb	2.9	2	0.7	2.3	0.9	0.7
Rb	17.5	18.5	29.6	55.8	46.2	0.2
Re	0.001	0.003	0.014	<0.001	0.026	<0.001
S	0.91	1.44	0.34	0.64	0.24	0.23
Sb	0.23	1.41	0.14	0.1	0.11	0.12
Sc	8.6	30.3	7.9	8.5	43.7	9.7
Se	1.4	1.4	0.8	0.7	0.6	0.6
Sn	0.3	0.2	<0.2	0.4	0.3	<0.2
Sr	52.6	105	50.4	38.3	53.7	89.6
Ta	<0.01	<0.01	<0.01	<0.01	<0.01	<0.01
Te	0.33	1.25	0.19	0.24	0.19	0.11
Th	1.8	<0.2	<0.2	2.3	<0.2	<0.2
Ti	0.068	0.084	0.102	0.227	0.168	0.046
Tl	0.13	0.12	0.18	0.38	0.24	<0.02
U	0.26	0.13	0.05	0.36	<0.05	0.07
V	75	219	74	76	235	165
W	0.21	1.24	0.14	1.08	14.45	0.71
Y	8.68	5.69	3.75	10.9	3.55	8.13
Zn	94	66	18	86	55	59
Zr	2.1	0.8	<0.5	3.6	<0.5	<0.5

Geochemically, correlation graphs plotted for Mn, Mg, Fe, Cu, and Ag in figure 4.5 showed vertical graphs. There is no correlation between gold and any of the elements plotted. This is because the six samples assayed, all reported below detection gold values, yielding a constant value of 0.1, presenting no variability between the gold and the other samples. Thus the vertical graphs.

To further understand the reasons for the below detection of Au in the selected rocks, the study of the variation in concentrations of trace elements in various types of samples as a guide to the location of mineral deposits in the area Ridgway et al. (1994) was explored. This was conducted by plotting the concentration of trace elements in the selected rock samples against the average abundance of trace elements in normal igneous rocks (Green, 1959) as shown in figure 4.5.

From the graphical plots shown in figure 4.5 and the table 4.3, Cr, Co, Sb, Sc, Te and V showed a higher average elemental abundance in the selected samples compared with the average abundance of element in a normal igneous rock. Major pathfinders to gold mineralization with the exception of As, however showed a lower average elemental abundance in selected rocks compared with the average abundance of elements in a normal igneous rocks. Even though the average abundance of As in the selected samples was higher compared with average elemental abundance of As in normal igneous rocks, As was predominant in samples ANDD036 and ANRC227 with average As values of 76.5 ppm and 58.5 ppm as against average elemental abundance of normal igneous rocks of 2ppm, the rest of the selected samples showed lower elemental abundance of Arsenic. According to Green, 1959, the concentrations of the trace elements in rock samples should be high above the concentration of these elements in normal igneous rocks before considered anomalous. Clearly so, the average abundance of trace elements with such as As, Mn, Fe, Cu, Mg and Ag in igneous rocks which are pathfinders to gold mineralization in the Birimian were below the background values of average elemental abundance of As,Mn,Fe,Cu,Mg and Ag in normal igneous rocks and were suggesting that the intrusive is not mineralized according to (Green,1959).

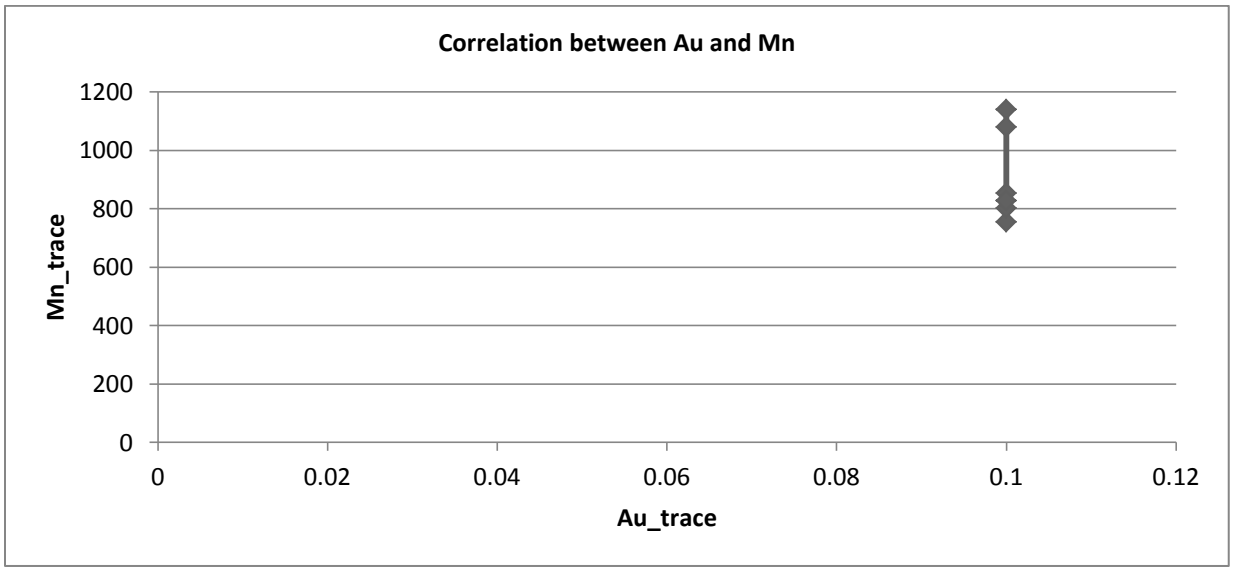

Figure 4.6: Correlation plot between Au against Mn

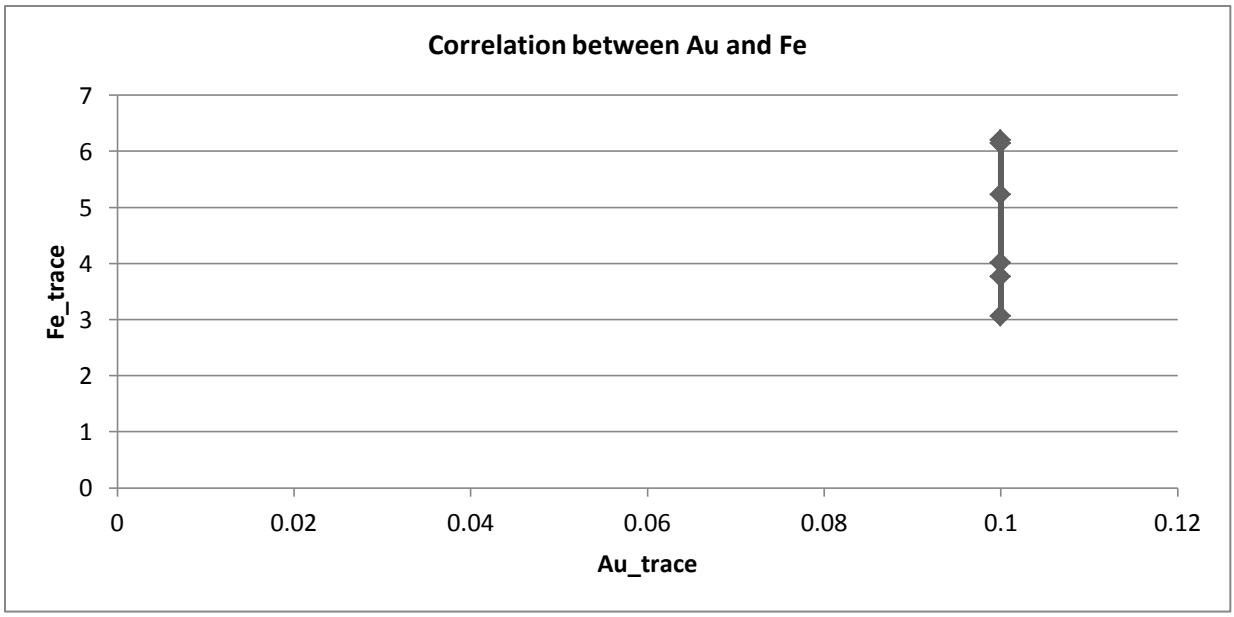

Figure 4.5: Correlation plot between Au against Fe

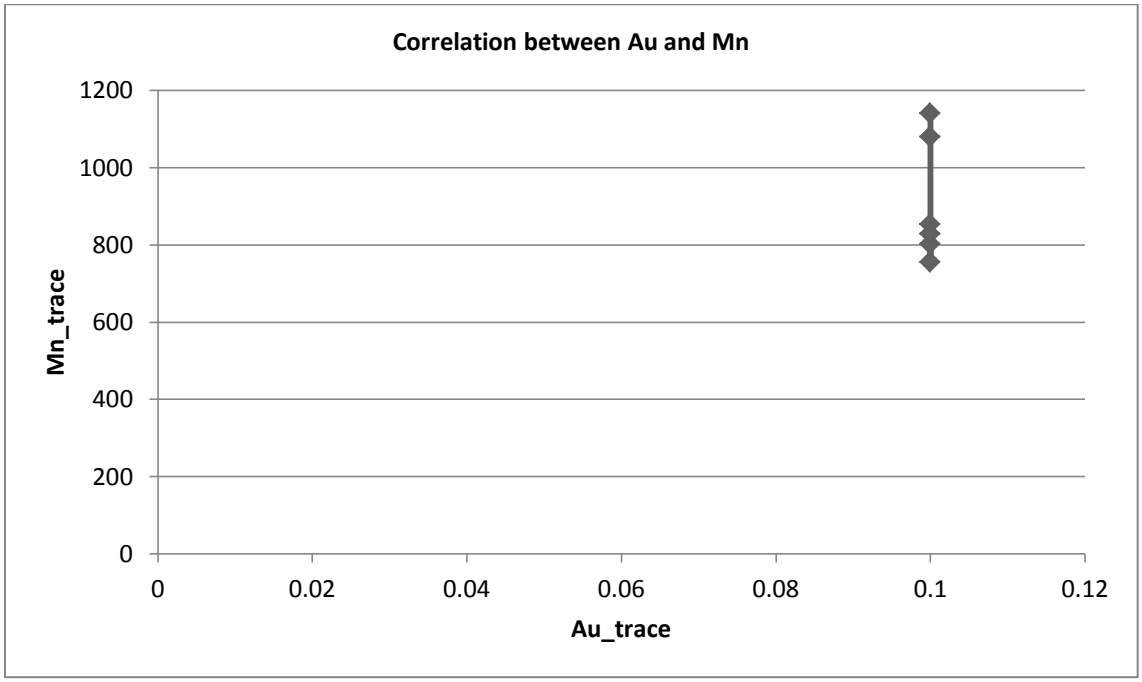

Figure 4.6: Correlation plot between Au against Mn

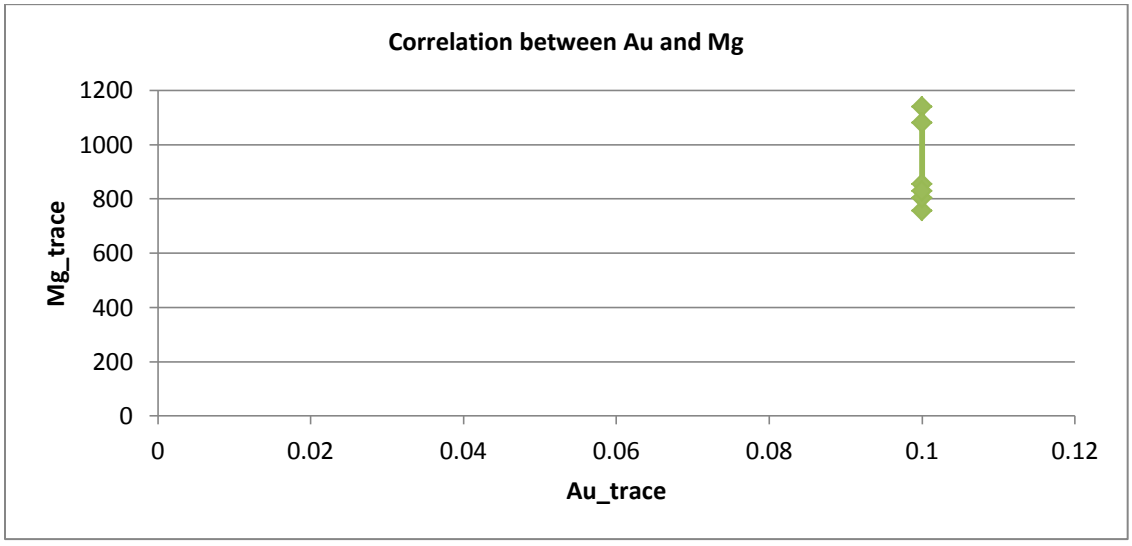

Figure 4.7: Correlation plot between Au against Mn

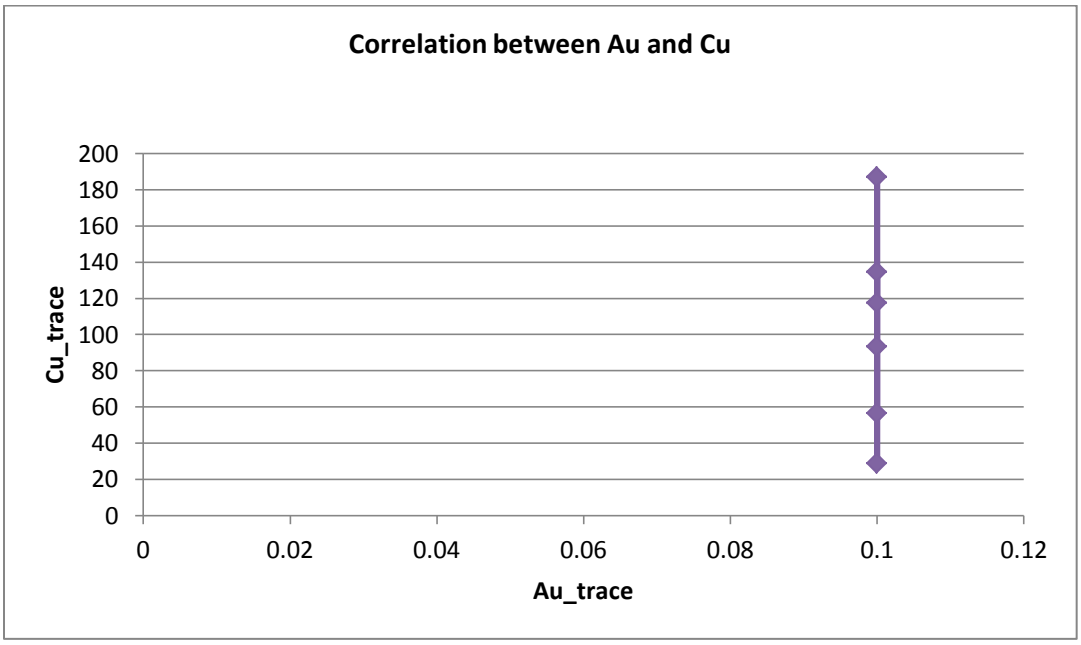

Figure 4.8: Correlation plot between Au against Cu

Table 4.6 showing Average abundance of selected rocks and Average abundance of elements in igneous rocks								
Elements	ANDD036	ANRC227D	ANRC232D	ANRC230D	ANRC228D	ANRC231D	Avg Abdnce in sltd Rks	Avg Abdce Igneous Rks,Green (1959)
Ag	0.13	0.2	0.06	0.06	0.14	0.06	0.108333333	0.2
Al	1.46	2.14	1.37	2.11	2.25	1.79	1.853333333	81000
As	76.5	58.5	0.9	1.1	1.2	0.9	23.18333333	2
Au	0.1	0.1	0.1	0.1	0.1	0.1	0.1	0.001
B	9	9	9	9	9	9	9	13
Ba	130	190	50	410	140	<10	184	640
Be	0.13	0.14	<0.05	0.11	0.06	<0.05	0.11	4.2
Bi	0.36	0.43	0.12	0.1	0.12	0.05	0.196666667	0.1
Ca	3.47	5.08	4.56	1.96	3.81	4.4	3.88	33000
Cd	0.07	0.1	0.03	0.03	0.07	0.03	0.055	0.13
Ce	25.2	4.46	2.18	40.5	3.41	4.22	13.32833333	40
Co	21.3	46.6	25.1	14.5	56.8	43	34.55	18
Cr	27	361	162	27	435	193	200.8333333	117
Cs	0.89	1.14	5.5	6.16	3.14	0.09	2.82	10
Cu	56.4	134.5	93.3	28.7	187	117.5	102.9	70
Fe	4.02	6.2	3.07	3.77	6.15	5.23	4.74	46500
Ga	5.69	7	3.4	9.09	8.11	6.46	6.625	26
Ge	0.08	0.12	0.17	0.11	0.22	0.19	0.148333333	2
Hf	0.06	0.03	0.02	0.11	<0.02	<0.02	0.055	3
Hg	<0.01	<0.01	<0.01	<0.01	0.01	<0.01	0.01	0.06
In	0.027	0.035	0.015	0.029	0.055	0.017	0.029666667	0.1
K	0.39	0.5	0.57	1.57	1.29	0.01	0.721666667	25000
La	12.8	2.2	0.8	19.4	1.2	1.6	6.333333333	20
Li	20.2	30.9	34.5	38.6	43.5	14.3	30.33333333	50
Mg	0.98	3.06	1.84	1.44	3.39	2.49	2.2	17000
Mn	1140	1080	755	853	802	828	909.6666667	1000
Mo	1.21	4.44	8.58	0.69	9.71	0.13	4.126666667	1.7
Na	0.04	0.03	0.07	0.05	0.04	0.04	0.045	25000
Nb	0.12	<0.05	<0.05	0.16	<0.05	<0.05	0.14	20
Ni	22.7	147	70.7	13.9	185	127	94.38333333	100
P	420	200	240	830	240	230	360	900
Pb	2.9	2	0.7	2.3	0.9	0.7	1.583333333	16
Rb	17.5	18.5	29.6	55.8	46.2	0.2	27.96666667	280
Re	0.001	0.003	0.014	<0.001	0.026	<0.001	0.011	0.001
S	0.91	1.44	0.34	0.64	0.24	0.23	0.633333333	900
Sb	0.23	1.41	0.14	0.1	0.11	0.12	0.351666667	0.3
Sc	8.6	30.3	7.9	8.5	43.7	9.7	18.11666667	13
Se	1.4	1.4	0.8	0.7	0.6	0.6	0.916666667	o.o1
Sn	0.3	0.2	<0.2	0.4	0.3	<0.2	0.3	32
Sr	52.6	105	50.4	38.3	53.7	89.6	64.93333333	350
Ta	<0.01	<0.01	<0.01	<0.01	<0.01	<0.01	#DIV/0!	2.7
Te	0.33	1.25	0.19	0.24	0.19	0.11	0.385	0.001
Th	1.8	<0.2	<0.2	2.3	<0.2	<0.2	2.05	13
Ti	0.068	0.084	0.102	0.227	0.168	0.046	0.115833333	1.7
Tl	0.13	0.12	0.18	0.38	0.24	<0.02	0.21	3
U	0.26	0.13	0.05	0.36	<0.05	0.07	0.174	2.6
V	75	219	74	76	235	165	140.6666667	90
W	0.21	1.24	0.14	1.08	14.45	0.71	2.971666667	2
Y	8.68	5.69	3.75	10.9	3.55	8.13	6.783333333	15
Zn	94	66	18	86	55	59	63	80
Zr	2.1	0.8	<0.5	3.6	<0.5	<0.5	2.166666667	170

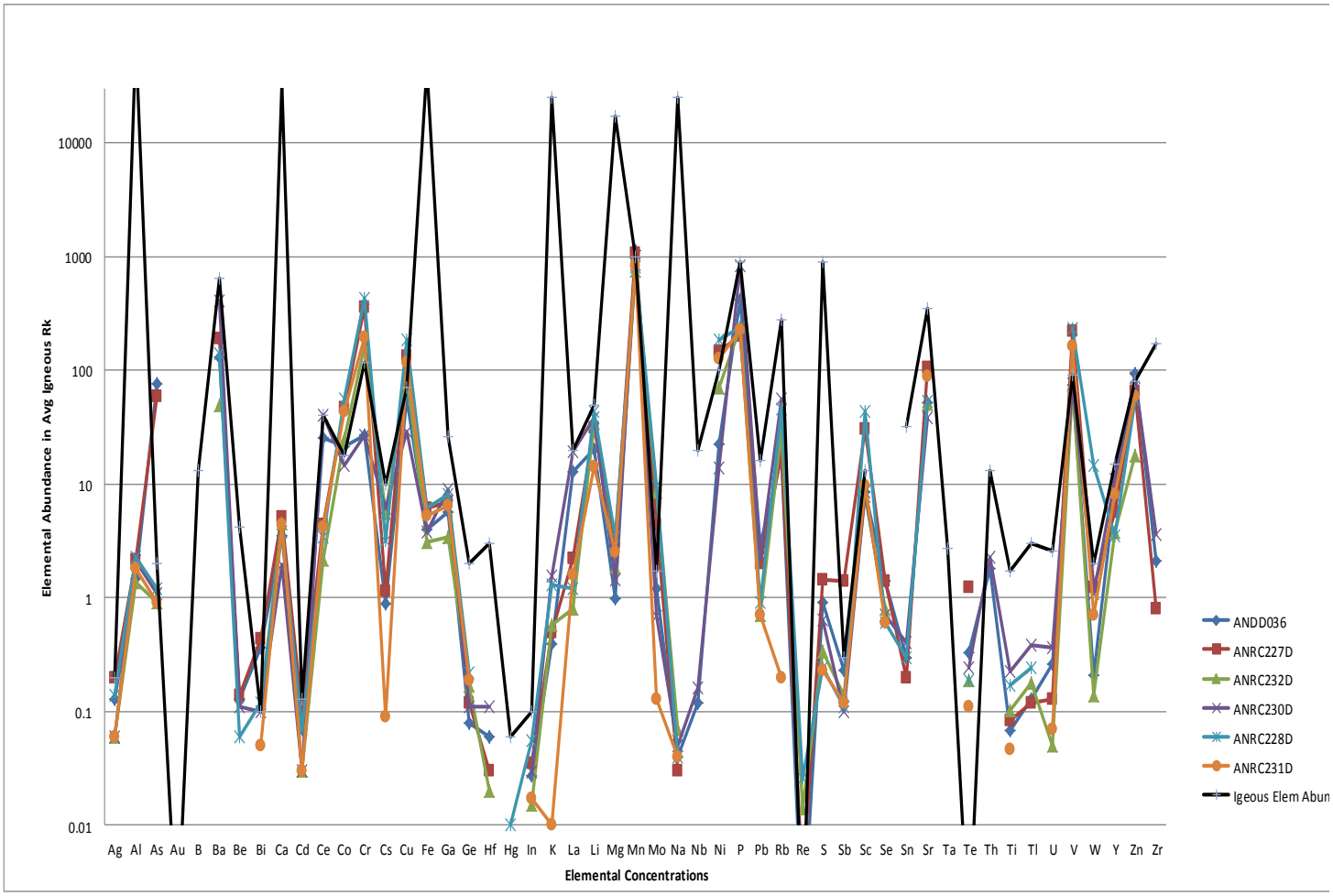

Figure 4.6: A plot of concentrations of trace elements in samples and concentrations of trace elements in normal rocks.

4.4 Discussions

The results of the investigation are discussed vis-à-vis the problems identified and contained in chapter 1, namely;

1. Geochemistry

2. Petrography

3. Structure

4.4.1 Geochemistry.

Reported values of Au are below detection limit. As industry practice in order to remove the less than sign, the values were divided by 0.2ppm

Geochemically, correlation graphs plotted for As, Mn, Mg, Fe, Cu, Ag showed vertical graphs (figures 4.6, 4.7, 4.8.4.9 in appendix 1) indicating no correlation between gold and any of the pathfinder elements plotted. This is because the six samples assayed, all reported below detection gold values, yielding a constant value of 0.1, presenting no variability between the gold and the other samples. Thus the vertical graphs.

To further understand the reason for the below detection plots the average concentration of trace elements (As, Mn, Mg, Fe, Cu, Ag) in the selected rocks as against the average abundance trace element (As, Mn, Mg, Fe, Cu, Ag) in normal igneous rock as seen in figure 4.5 and table 4.3 also showed that the concentration of average abundance of major pathfinders to gold mineralisation were below the background values of normal igneous rocks suggesting the rock is unmineralised.

4.4.2 Petrography

Four unique intrusive namely, Meta Gabbro, Meta Diorite, Grano Diorite and Meta Dolerite were identified petrographically as shown in figure 4.1,4.2,4.3 and 4.4. These were however grouped into two rock types based

on their petrographic compositions; the Meta dolerite and Meta Diorite. Meta Gabbro, Meta Diorite and Grano Diorite were collectively grouped as the diorite based on their composition and texture diorite.

The Dolerite specimens are fine to medium grained suggesting the magma cooled close to surface whereas diorite specimen are medium to coarse grain suggesting magma cooled at depth.

It can be seen from the photomicrographs in Figure. 4.2 and 4.3 that Plagioclase is subhedral to euhedral porpheries and slightly altered to sericite. Calcite appears as isolated aggregates, might be probably secondary and interstitial. Epidote appears elongated and acicular. These two minerals may have been altered from the primary ferromagnesian minerals such as pyroxene and amphiboles probably hornblende as pseudomorphs. The sericite could be an altered product of plagioclase. The alteration assemblage of rock samples contains varying proportions of muscovite/sericite, tourmaline and quartz is suggestive that rocks are of Greenshist facies and is as a result of reaction with strongly reducing fluids. Low level addition of chlorite-chloritisation and development of pyrite-pyritisation shows the effects of near surface temperature and pressure regimes.

Carbonate occurs only as veins and therefore could only be described as secondary. Rocks had little or no carbonate in the unmineralised intrusive compared with the mineralized igneous rocks at the Greater Damang project area. The presence of carbonate- fluids is suggestive of the mineral of hydrothermal origin.

Although most of the quartz is thought to be an alteration product it is thought that some could represent remnant igneous quartz from a quartz diorite.

The introduction of silica and alteration of primary quartz into secondary quartz through silicification is seen in photomicrographs shown in Figures 4.1, 4.2, 4.3. In some instances quartz veins and veinlet's develop filling existing fractures. The extent of silification in dioritic igneous rocks of greater Damang as shown in figure 4.7 is predominant compared with dioritic rocks at Amoanda project area in figure 4.1, 4.2, and 4.3. This is evident of the fact that hydrothermal fluids flowed through the rocks. Pyrite, pyrohtite, chalcopyrite and magnetite happens to be the major alteration minerals in the mineralized rock whereas chlorite, sericite and cubic pyrites

are presents in the unmineralised igneous rocks. Pyrite in the unminiralised intrusives are cubic in nature but that of the mineralized are euhedral shaped suggesting a change in the original shape of the minerals due to extensive deformation from its original subhedral shape. Tiny gold grains are observed to have grown within the euhedral pyrite cystals. This suggests that the gold grains are younger than pyrite in the mineralized intrusive and might have been deposited out of an ore-bearing hydrothermal fluid.

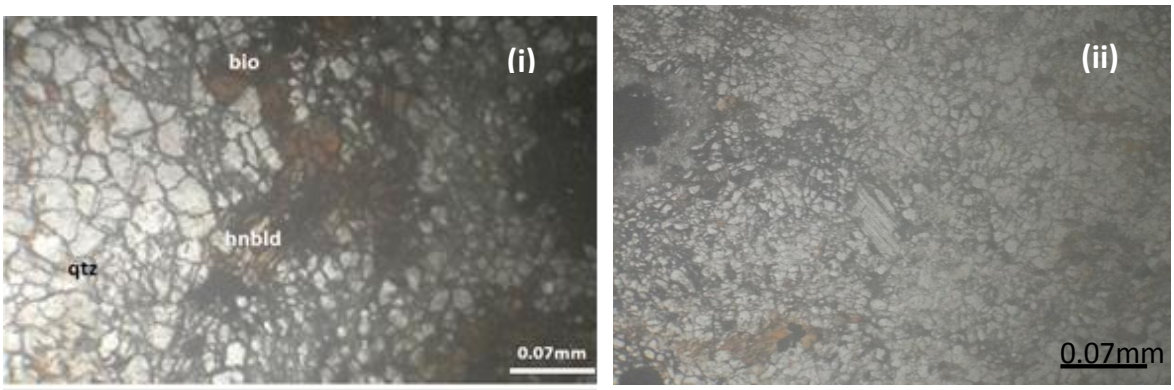

Figure 4.9 (i & ii): Photomicrographs of specimen from Greater Damang showing fractured quartz and columnar hornblende.

4.4.3 Structure

The mafic intrusives are affected by tectonic events in the area. This is evident by the weak fracturing as shown in Fig. 4.1, 4.2 and 4.3. Also, photomicrographs in Fig. 4.1, 4.2 and 4.3 shows elongated, acicular and shredded epidote, threadlike muscovite and fractured quartz, which also suggests that the rocks have suffered a structural deformation. Calcite appears as isolated aggregates, might be probably secondary. These secondary or post-emplacement fractures appear to have served as conduits, creating the needed space for the passage for hydrothermal fluids. Conduits created however are not extensive.

Deep-seated dioritic intrusive at the greater Damang however are extensive due to the fact that the area been affected by prominent northeast-southwest structures as shown in figure 4.8 below. The presence of the prominent structures provided the enabling environment for the permeation, cooling and subsequent deposition of gold mineralization from ore-bearing hydrothermal fluids.

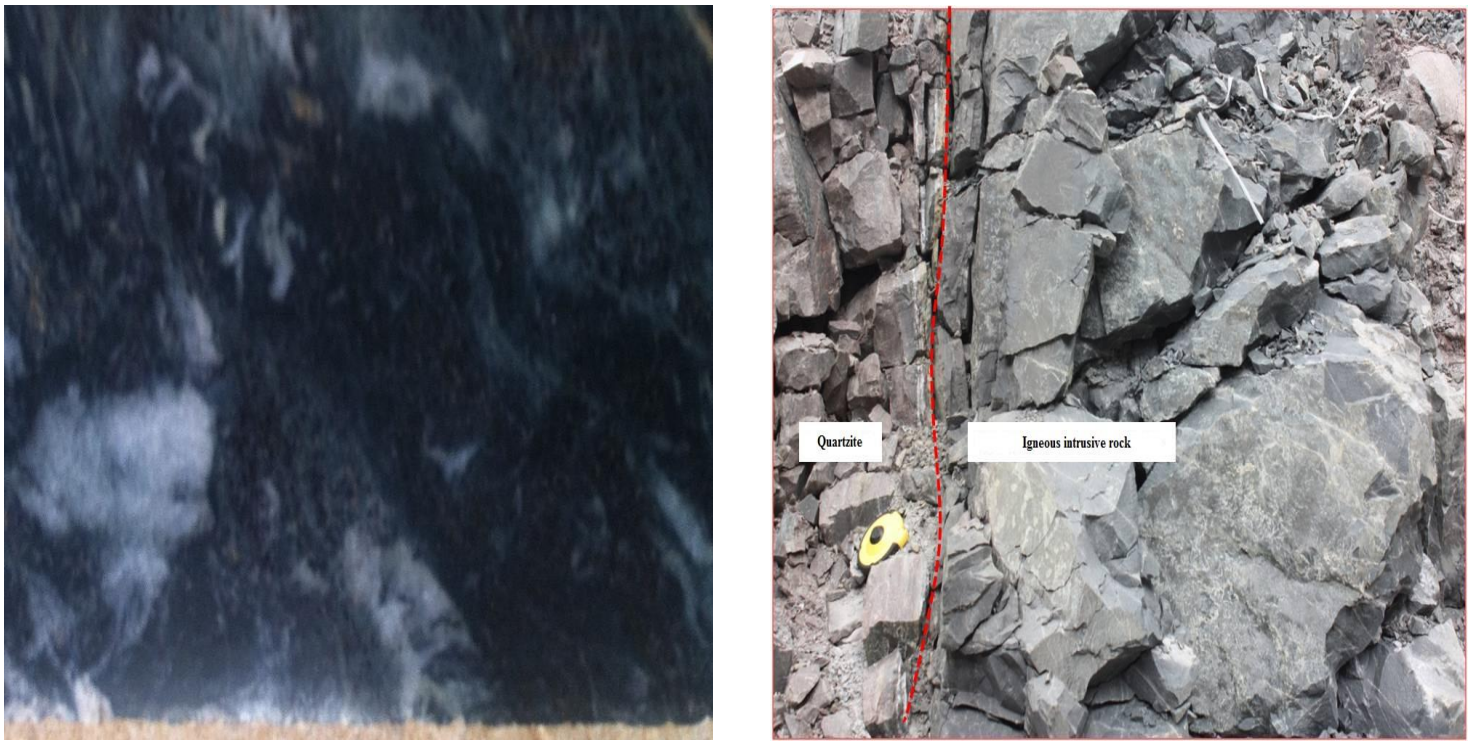

Figure 4.10 (A) **Photomicrograph of Amoanda showing weak deformation (B) rocks from Greater Damang showing extensive deformation.**

CHAPTER FIVE

CONCLUSION AND RECOMMENDATIONS

5.1 Conclusion

The outcome of this research shows that the Greater Amoanda project area has two unique igneous rocks, namely the Meta Diorite and Meta Dolerite

The major differences however between the diorite mineralized and the unmineralised diorites in the two project area are below:

1. Petrography; Whiles two unique igneous intrusives (the Meta Dolerite and Meta Diorite) are present in Amoanda project area, only diorite outcrops at the greater Damang project area. The dolerites are fine to medium grained whereas the diorite is medium to coarse grained. This point to the fact that the rock-forming magma cooled at different depths or horizons.

2. Geochemically; From the trace elements plot, the average abundance of trace elements with specific mention to As, Mn ,Fe ,Cu ,Mg and Ag in igneous rocks which are pathfinders to gold mineralisationin in the Birimian were below the background values of average elemental abundance of As, Mn ,Fe ,Cu ,Mg and Ag in normal igneous rocks suggesting that the intrusives in the Amoanda project area is unmineralised.

3. Alteration; Mineralised igneous intrusive rocks at the greater Damang are highly silicified compared with the unmineralised intrusive rocks at Amoanda. Carbonates occur only as veins and are predominant in mineralized dioritic rocks but little or no carbonation in the unmineralised intrusive rocks.

The major alteration minerals in the mineralized rocks are pyrite, pyrohtite, chalcopyrite and magnetite whereas chlorite, sericite and cubic pyrites are presents in the unmineralised igneous Pyrite in the unminiralised intrusives are cubic in nature but that of the mineralized are euhedral shaped suggesting a change in the original shape of the minerals due to extensive deformation from its original subhedral shape. Tiny gold grains are

observed to have grown within the euhedral pyrite crystals. It can therefore be concluded that gold bearing dioritic intrusives have higher abundance of carbonates minerals and euhedral shaped pyrites compared with the unmineralised igneous rock in which cubic pyrites and little or carbonates.

4. Structure; Igneous dioritic rocks at Amoanda project areas are weakly foliated and slightly sheared and whereas mineralized intrusive are extensively deformed. The extensive deformation of mineralized deep seated igneous rocks may be as a result of the presence of a structural regime that ruptured and provided enabling environments for the permeation, cooling and subsequent deposition of gold mineralization from the ore bearing hydrothermal fluids.

5.2 Recommendation

It is recommended that further research be carried out on the mafic intrusive rocks using large sample size and as mining activities continue and advance, extensive pit mapping be done to delineate and analyse the diorite intrusive and their associated structures and alterations with more emphasis on zones that are highly rich in carbonate veins and disseminated pyrites.

REFERENCES

Abouchami, W., Boher, M., Michard, A., Albarede, F., 1990. A major 2.1 Ga event of mantle magmatism in West Africa: an early stage of crustal accretion. J. Geophys. Res. 95, 17605–17629.

Albarède, F., Brouxel, M., 1987. The Sm–Nd secular evolution of the continental crust and the depleted mantle. Earth Planet. Sci. Lett. 82, 25–36.

Ama-Salah, I., Liegeois, J.-P., Pouclet, A., 1996. Evolution d'un arc insulaireocéaniquebirimianprécoce au Liptakonigérien (Sirba): géologie, géochronologie et géochimie. J. Afr. Earth Sci. 22 (3), 235–254.

Asiedu, D.K., Dampare, S.B., Asamoah, S. P., Banoeng-Yakubo, B., Osae, S., Nyarko, B.J.B., Manu, J., 2004. Geochemistry of Paleoproterozoicmetasedimentary rocks from the Birim diamondiferous field, southern Ghana: Implications for provenance and crustal evolution at the Archean-Proterozoic boundary. Geochem. J. 38, 215-228.

Asihene, K.A.B., Barning, K., 1975. A contribution to the stratigraphy of the Birimian System of Ghana, West Africa. Ghana Geol. Survey Report 75/5, Accra, 30 pp.

Bach, W., Hegner, E., Erzinger, J., 1998. Chemical fluxes in the Tonga subduction zone: evidence from the southern Lau Basin. Geophys. Res. Lett. 25, 1467–1470.

Boher, M., Abouchami, W., Michard, A., Albarède, F., Arndt, N.T., 1992. Crustal growth in West Africa at 2.1 Ga. J. Geophys. Res. 97, 345–369.

Bonatti, E., Michael, P.J., 1989. Mantle peridotites from continental rifts to ocean basins to subduction zones. Earth Planet. Sci. Lett. 91, 297–311.

Bonhomme, M., 1962. Contribution à l'étude géochronologique de la plate-forme de l'Ouest africain. Géologie et Minéralogie, vol. 5. Thesis. University of Clermont-Ferrand, Fr., p. 62.

Bossière, G., Bonkoungou, I., Peucat, J.J., Pupin, J.P., 1996. Origin of Paleoproterozoic conglomerates and sandstones of the Tarkwaian Group in Burkina Faso, West Africa. Precambrian Res. 80, 153–172.

Bourgois, J., Desmet, A., Tournon, J., Aubouin, J., 1985. Mafic and ultramafic rocks of Leg 84:

49.

Cudjoe, J.E., 1962. The geology of 1/4° field sheet 7. Ghana Geol. Surv. Rep., 113 pp.

Dampare, S., Shibata, T., Asiedu, D., Osae, H., 2005. Major-element geochemistry of Proterozoic Prince's Town granitoid from the southern Ashanti volcanic belt, Ghana. Okayama Univ. Earth Sci. Reports 12, 15–30.

Dampare, S.B., Shibata, T., Asiedu, D.K., Osae, S. and Banoeng-Yakubo, B., in press. Geochemistry of Paleoproterozoicmetavolcanic rocks from the southern Ashanti volcanic belt, Ghana: petrogenetic and tectonic setting implications. Precambrian Res. DOI: 10.101/j.precamres.2007.10.001.

Davis, D.W., Hirdes, W., Schaltegger, U., Nunoo, E.A., 1994. U-Pb age constraints on deposition and provenance of Birimian and gold-bearing Tarkwaian sediments in Ghana, West Africa. Precambrian Res., 67, 89–107.

Eisenlohr, B.N., 1989. The structural geology of Birimian and Tarkwaian rocks of southwest Ghana. Rep. Arch. BGR, 66 pp.

Eisenlohr, B.N., Hirdes, W., 1992. The structural development of the early Proterozoic Birimian and Tarkwaian rocks of southwest Ghana, West Africa. J. Afr. Earth Sci. 14, 313–325.

Feybesse, J.L., Billa, M., Guerrot, C., Duguey, E., Lescuyer, J.L., Jean-Pierre Milési, J.P., Bouchot, V., 2006. The paleoproterozoic Ghanaian province: geodynamic model and ore controls, including regional stress modeling. Precambrian Res. 149, 149–196.

Feybesse, J.L., Milési, J.P., 1994. The Archean/proterozoic contact zone in West Africa: a mountain belt of décollement thrusting and folding on a continental margin related to 2.1 Ga convergence of Archeancratons? Precambrian Res. 69, 199–227.

Hirdes, W., Davis, D.W. and Eisenlohr, B.N., 1992. Reassessment of Proterozoic of Proterozoic granitoid ages in Ghana on the basis of U/Pb zircon and monzanite dating. Precambrian Res. 56, 89-96.

Hirdes, W., Davis, D.W., 2002. U–Pb geochronology of Paleoproterozoic rocks in the southern part of the Keougou-Keneba inlier, Senegal, West Africa: evidence for diachronousaccretionary development of the Birimian Province. Precambrian Res. 118, 83–99.

Hirdes, W., Nunoo, B., 1994. The Proterozoic paleoplacers at Tarkwa gold mine, SW Ghana: sedimentology, mineralogy, and precise age dating of the Main Reef and West Reef, and bearing of the investigations on source area aspects. Geologisches Jahrbuch, D100, 247–311.

Hirdes, W., Senger, R., Adjei, J., Efa, E., Loh, G., Tettey, A., 1993. Explanatory notes for the geological map of southwest Ghana: 1:1000000. GeologischesJahrbuch, 83, 5–139.

Hirdes,W., Davis, D.W., Lüdtke, G., Konan, G., 1996. Two generations of Birimian (Paleoproterozoic) volcanic belts in northeastern Côte d'Ivoire (West Africa): consequences for the 'Birimian controversy'. Precambrian Res. 80, 173–191.

Hirst, T., 1935. Gold prospects in the Axim-Sekondi District, Gold Coast. Ann. Rep. Gold Coast Geol. Surv., pp. 23–24.

Junner, N.R., 1935. Gold in the Gold Coast. Mem. Gold Coast Geol. Surv., 4, 67 pp.

Junner, N.R., 1940. Geology of the Gold Coast and Western Togoland. Gold Coast Geol. Surv. Bull. 11, 40 pp.

Junner, N.R., Hirst, T., Service, H., 1942. The Tarkwa Goldfield. Gold Coast Geol. Surv., 6, 75 pp.

Kesse, G.O., 1985. The mineral and rock resources of Ghana. Balkema, Rotterdam, 610 pp.

Kitson, A.E., 1918. Ann. Rep. Geol. Surv. Gold Coast for 1916/17. Accra.

Kitson, A.E., 1928. Provisional geological map of the Gold Coast and Western Togoland, with brief notes thereon. Gold Coast Geological Survey Bull No. 2, 13 pp.

Klemd, R., Hirdes, W., Oleesch, M., Oberthür, T., 1993. Fluid inclusion in quartz-pebbles of the gold-bearing Tarkwaian conglomerates of Ghana as guides to their provenance area. Miner. Deposita 28, 334–343.

Ledru, P., Milesi, J.-P., Vinchon, C., Ankrah, P.T., Johan, V., Marcoux, E., 1988. Geology of the Birimian series of Ghana. In: International Conference and Workshop on the Geology of Ghana with Special Emphasis on Gold Programme and Abstracts, Accra, Ghana, pp. 26-27.

Leube, A., Hirdes, W., Mauer, R., Kesse, G.O., 1990. The early Proterozoic BirimianSupergroup of Ghana and some aspects of its associated gold mineralization. PrecambrianRes. 46, 139–165.

Liégeois, J.P., Claessens, W., Camara, D., Klerkx, J., 1991. Short-lived Eburnian orogeny in southern Mali. Geology, tectonics, U–Pb and Rb–Sr geochronology. Precambrian Res. 50, 111–136.

Loh, G., Hirdes, W., 1999. Explanatory notes for the geological map of southwest Ghana 1:100,000: sheets Sekondi (0402A) and Axim (0403B): Ghana. Geol. Surv. Bull. 49, 149 pp.

Milési, J.P., Ledru, P., Feybesse, J.L., Dommanget, A., Marcoux, E., 1992. Early Proterozoic ore deposits and tectonics of the Birimianorogenic belt, West Africa. Precambrian Res. 58, 305–344.

Miyashiro, A., 1974. Volcanic rock series in island arcs and active continental margins. Am. J. Sci. 274, 321–355.

Nelson, B.K., DePaolo, D.J., 1984. 1,700-Myr greenstone volcanic successions in southwestern North America and isotopic evolution of Proterozoic mantle. Nature, 312, 143–146.

Nelson, B.K., DePaolo, D.J., 1985. Rapid production of continental crust 1.7 to 1.9 b.y. ago: Nd isotopic evidence from the basement of the North America mid continent. Geol. Soc. Am.

Pigois, J.-P., Groves, D.I., Fletcher, I.R., McNaughton, N.J., Snee, L.W., 2003. Age constraints on Tarkwaianpalaeoplacer and lode-gold formation in the Tarkwa-Damang district, SW Ghana. Miner. Deposita 38, 695–714.